# The Spatial Deployment of Renewable Energy Based on China's Coal-heavy Generation Mix and Inter-regional Transmission Grid

*Bo-Wen Yi,*[a] *Wolfgang Eichhammer,*[b] *Benjamin Pfluger,*[c] *Ying Fan,*[d] *and Jin-Hua Xu*[e]

**ABSTRACT**

China has set a goal of 20% non-fossil energy in total primary energy consumption by 2030. The decision of where to invest in renewable energy, and to what extent, needs to be considered from a forward-looking perspective. This article presents a power sector optimization model that integrates unit commitment with long-term generation expansion planning framework. Power dispatches at an hourly level are combined with yearly investment decisions. Based on the model, this article analyzes the optimal spatial deployment of renewable energy. The results show that regional differences in non-hydro renewable energy are significant. Approximately 75% should be deployed in the north of China. With the increase of combined heat and power, more renewable energy facilities, especially solar photovoltaic, should be located in the south of China. Inter-regional power transmission is beneficial to onshore wind in resource-rich areas, and could mitigate the conflict between coal-heavy generation mix and renewable energy.

**Key words:** Renewable energy, Power sector, CHP, Inter-regional power transmission

https://doi.org/10.5547/01956574.40.4.bwyi

## 1. INTRODUCTION

Increasing the utilization of renewable energy is crucial to coping with climate change. As the world's largest $CO_2$ emitter, China has realized the importance of developing renewable energy, and in the U.S.-China Joint Announcement on Climate Change set a target of 20% non-fossil fuels in primary energy consumption (renewables and nuclear energy) by 2030 (XNA, 2014). Renewable energy investment is highly capital-intensive, and once built, it creates a "lock-in" effect on the power generation mix for decades. Thus, whether the future low-carbon goals can be achieved depends on the current power system layout. The decision of where to invest in renewable energy, and to what extent, needs to be considered from a forward-looking perspective.

However, there are significant differences in resource endowments and electricity demand from region to region in China. Geographically, the potential for renewable energy is greatest in the

[a] School of Economics & Management, Beihang University, Beijing 100191, China, E-mail: ybw2018@buaa.edu.cn.

[b] Fraunhofer Institute for Systems and Innovation Research, Karlsruhe 76139, Germany, E-mail: Wolfgang.Eichhammer@isi.fraunhofer.de; and Utrecht University, Copernicus Institute of Sustainable Development, 3584 CB Utrecht, The Netherlands.

[c] Fraunhofer Institute for Systems and Innovation Research, Karlsruhe 76139, Germany, E-mail: Benjamin.Pfluger@isi.fraunhofer.de.

[d] Corresponding author. School of Economics & Management, Beihang University, Beijing 100191, China. E-mail: yfan1123@buaa.edu.cn.

[e] Corresponding author. Center for Energy and Environmental Policy Research, Institutes of Science and Development, Chinese Academy of Sciences, Beijing 100190, China. E-mail: xujinhua111@163.com.

*The Energy Journal*, Vol. 40, No. 4. Copyright © 2019 by the IAEE. All rights reserved.

north of China, while the power demand in the east and south is higher due to advanced economic development in those regions. The imbalance of resource endowments and electricity loads makes the spatial deployment of renewable energy more difficult.

In the north of China, a coal-heavy power supply structure limits the possibilities for integrating further renewable energy into the power grid. The large-scale application of coal-fired combined heat and power (CHP) has led to serious wind curtailment problems during winter, with a curtailment rate of 20.6% in 2016 (NEA, 2017). Compared with traditional coal-fired units, CHP unit operation is more inflexible because it must generate electricity when providing heating supply. During the winter, high heating demand in the north of China forces the CHP plants in district heating grids into must-run mode. The regional conflicts between the existing power generation mix and renewable energy are significant. Yet, with the increase of ultra-high voltage technology, inter-regional power transmission may be conducive to the consumption of renewable energy. Consequently, both the coal-heavy generation mix and inter-regional transmission planning affect the optimal spatial deployment of renewable energy.

The deployment of renewable energy at the spatial level in a manner that achieves stringent low-carbon target cost efficiency is of particular concern to China. Dong et al. (2016) conducted an empirical analysis of the distribution and cluster patterns of the country's renewable energy industry. Zhang et al. (2017) examined the regional development status of renewable energy, and made projections for the future expansion of renewables in China. Pei et al. (2015) analyzed wind curtailment problems from a temporal-spatial perspective. Their results showed that the present coal-wind-nuclear power structure in the north of China is one of the main reasons for curtailment. Based on the current literature, we find there is a need to implement comprehensive energy planning to analyze the spatial deployment of renewable energy and its related influencing factors.

However, describing fluctuating renewable energy in the energy system model is complicated, because it requires a relatively high-frequency temporal resolution, generally based on hours. Traditional power generation expansion planning (GEP) models are widely applied for energy planning from a bottom-up perspective (Bird et al., 2011; Sullivan et al., 2014; Wright and Kanudia, 2014; Chang and Li, 2015; Li and Chang, 2015). However, these models often simplify the fluctuating and seasonal features of renewable energy, and ignore the dispatch characteristics of generation units, such as ramping limits and start-up and shut-down decisions. These are typically addressed by unit commitment (UC) models (Kaleta and Toczyłowski, 2008; Keane et al., 2011; Weigt el al., 2013; Egerer et al., 2015; Moarefdoost el al., 2016). Few studies integrate short-team power dispatch decisions into a long-term GEP framework (Koltsaklis and Georgiadis, 2015; Abrell and Rausch, 2016; Egerer et al., 2016; Bertsch et al., 2017). Pfluger (2014) expanded the electricity system model PowerACE to assess least-cost pathways for decarbonizing Europe's power supply. Scholz et al. (2017) used high temporal and spatial resolution information in an integrated assessment model (IAM) to understand the potential contribution of concentrating solar power to the balancing of renewable energy in Europe. Perez et al. (2016) used a co-optimization planning model to quantify the economic effects of trading renewable energy certificates among the U.S. states.

In the Chinese context, Li et al. (2016) simulated the Chinese power sector in 2030 based on an UC model, which models the dispatch of six regional power grids at hourly intervals. Guo et al. (2017) integrated seasonal and diurnal temporal variations into a GEP framework by dividing one year into twelve time-blocks. Chen et al. (2018) expanded to ninety-six time-blocks based on Guo et al. (2017) to capture the impact of different charging modes of electric vehicles on power system investment. He et al. (2016) presented a high-resolution integrated model that optimizes

All rights reserved. Copyright © 2019 by the IAEE.

both the long-term investment and the short-term dispatch, but did not consider the characteristics of CHP.

To better understand the spatial deployment of renewable energy in China, this article makes three significant improvements compared to previous literatures by: (1) integrating hourly features of power dispatch, especially ramping limits, into traditional GEP model, which enables analyzing the impact of short-term power dispatch on long-term capacity investment; (2) modeling China's unique CHP operation mode in the energy system model to characterize the conflict between central heating supply and low-carbon energy transformation; and (3) analyzing the renewable energy deployment from a systematic perspective, which enables us to understand the inherent mechanism between power generation mix, power grid planning, and the large-scale utilization of renewable energy. Based on this framework, this study addresses two research questions: (1) what is the optimal spatial deployment of renewable energy to achieve relevant low-carbon targets? And (2) what are the effects of a coal-heavy generation mix and electricity transmission infrastructure expansion on the spatial deployment of renewable energy in China? Based on the analysis, policy recommendations will be developed for the Chinese government to make long-term strategic decisions about renewable energy deployment.

This paper is organized as follows. Section 2 provides a description of the conceptual framework. The detailed modeling, data, and scenario designs are presented in Section 3. Section 4 discusses the effects of a coal-heavy generation mix and electricity transmission infrastructure expansion on the spatial deployment of renewable energy. Section 5 presents the conclusions and recommendations.

## 2. CONCEPTUAL FRAMEWORK

### 2.1 Coal-heavy Generation Mix

Coal is the most important resource for power generation in China. In 2016, the proportion of the installed capacity of coal-fired power units was 57.3%. Coal power plants have more restrictive operational requirements than gas-fired power plants; for example, their ramping is slower. Furthermore, China has a large number of coal-fired CHP units providing district heating that cannot be shut down or easily modulated during the winter heating periods, which limits the flexibility of the power supply. The capacity of CHP reached 283 GW in 2014, accounting for 34% of the total coal-fired capacity (CEPYEB, 2015). In the Northern China and Northeast China power grids, the proportion exceeds 50%.

Figure 1 explains why the above-mentioned inflexible generation mix conflicts with renewable energy through an hourly electricity supply and demand curve. The difference between the daily load curve and the must-run capacity is the potential for other generation units. In an extreme case, even if no other units are dispatched, the amount of available renewable energy alone may exceed the above residual load, causing a renewable energy curtailment problem, especially for wind power. The feed-in profile of wind is typically high in winter mornings, while at this time the load curve is at the lowest point of the day. Due to this hourly mismatch of supply and demand, it is necessary to introduce a power dispatch model integrated with a power expansion model to better characterize renewable energy.

### 2.2. Inter-regional Electricity Trade

First, a stylized two-region model for electricity trade is presented as a reference for our empirical analysis (see Figure 2). Regions *A* and *B* are characterized by marginal cost supply curves

Copyright © 2019 by the IAEE. All rights reserved.

**Figure 1: Generation Mix and Renewable Energy Curtailment**

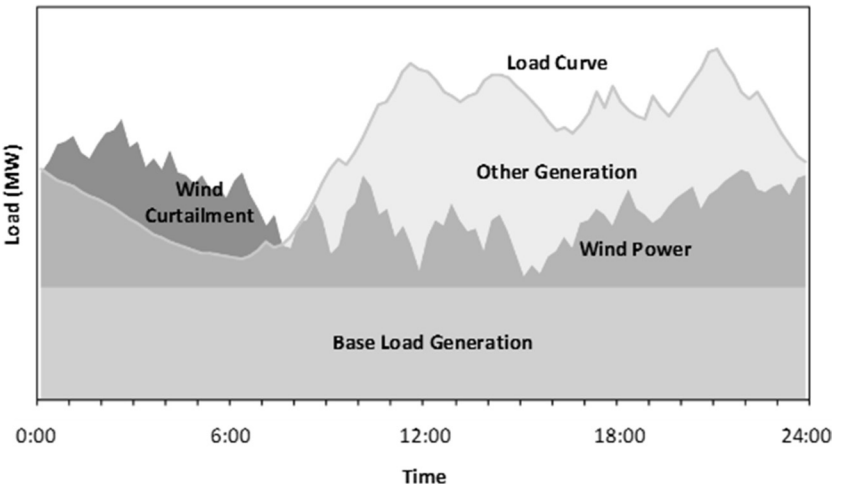


**Figure 2: Electricity Supply, Demand and Inter-regional Trade**

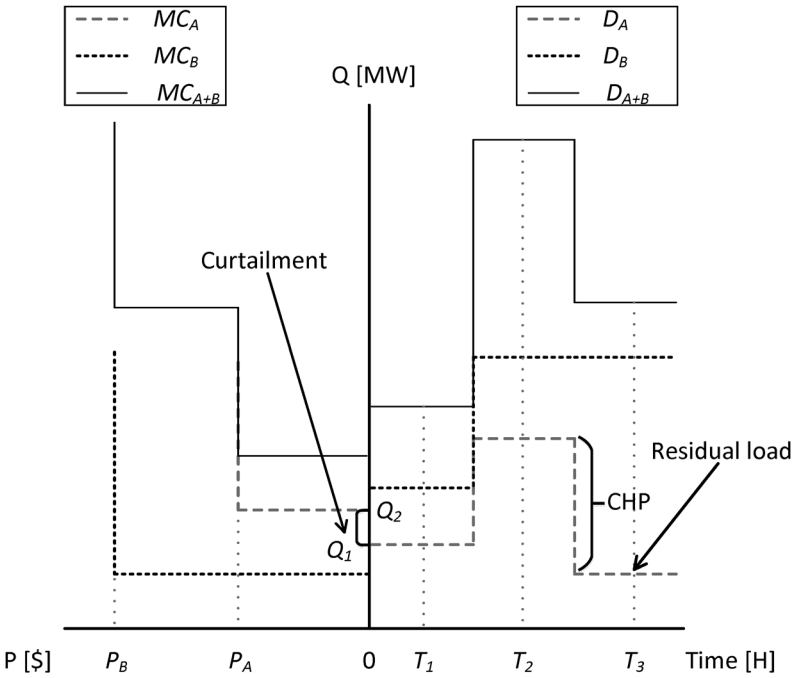


($MC_A$ and $MC_B$) and demand curves ($D_A$ and $D_B$). The step-wise supply curve is assumed to include two technologies: renewable energy with zero marginal cost and thermal power with different marginal costs $P_A$ and $P_B$. Region *A* approximates the electricity supply characteristics of Northwest China, where thermal power is relatively cheaper and renewable energy has greater potential. In contrast, Region *B* reflects the characteristics of East China. Through mapping the demand curves to the supply curves, we can find the equilibrium electricity price and trade amount at a given time.

In time $T_1$, without regional trade, regions *A* and *B* meet demand at the equilibrium prices of zero (region *A*) and $P_B$ (region *B*). If inter-regional trade is made possible, regardless of the

All rights reserved. Copyright © 2019 by the IAEE.

power transmission costs, the equilibrium price becomes $P_A$ by mapping $MC_{A+B}$ and $D_{A+B}$. Region $A$ becomes an electricity exporter and more renewable energy ($Q_2-Q_1$) is consumed due to the trade. But, electricity trade can increase the utilization of renewable energy mainly in situations of regional over-supply. For example, there is still a large amount of electricity traded from region $A$ to $B$ in time $T_2$, but renewable energy production is unchanged because demand is already higher than renewable energy supply in region $A$.

Due to central heating demands in the north of China, CHP effectively must operate at must-run capacity during winter. This can be represented in the model by lowering regional electricity demand to represent residual load (i.e. load supplied by non-baseload generators). Such a process is shown in Figure 2 by comparing $T_3$ to $T_2$ while decreasing demand in region $A$. The increase of must-run CHP results in renewable energy curtailment if there is no inter-regional transmission infrastructure; electricity trade could potentially lower or avoid this curtailment.

The purpose of this simple analysis is to illustrate the impact of electricity transfer and CHP on renewable energy. However, the influenced areas and the extent of the effects still need to be evaluated from the perspective of the national power system.

## 3. METHODOLOGY

### 3.1. Model Description

#### *3.1.1. Model Description and Assumptions*

This study presents a power sector optimization model that integrates unit commitment into a long-term generation expansion planning framework. The illustrative structure of our model is shown in Figure 3. Hourly power dispatch, taking into account characteristics such as ramping limits and start-up and shut-down decisions, is combined with yearly investment decisions for power generation and transmission technologies. In our previous work, we established a multi-region power GEP model to quantify the inter-regional power network (Yi et al., 2016; 2019). However, this model could not describe the fluctuating and seasonal features of renewable energy, and ignored the dispatch of generation units. This study therefore modifies the previous model by adding an hourly-based power dispatch model.

The power generation expansion module makes an investment decision at the beginning of each year to decide whether to build new generators and transmission lines. The power dispatch module optimizes hourly operations during the year based on the capacity determined by the power generation expansion module. The model minimizes the total system-wide costs of meeting electricity demand and renewable energy development constraints. The examined planning horizon is 2015–2030. Six typical days at an hourly level are considered within one year. The primary outputs include the least-cost power generation mix, inter-regional transmission networks, hourly electricity output, and carbon dioxide emissions.

The typical day method has been widely used in large-scale energy system models to cut back on temporal resolution and coverage. For example, the model applied in Lienert and Lochner (2012) considered four seasons, with each season including three typical days using a time step of two hours. Twelve typical days were applied in Koltsaklis and Georgiadis (2015), each representing a one-month period. Due to computational limitation, one year consists of six typical days in our model. Each typical day represents two consecutive months to reflect seasonal characteristics. Further, each day is subdivided into 24 one-hour periods. Thus, a one-year period consists of 144 temporal steps. These temporal steps are assumed to be consecutive. The committed capacities of

Copyright © 2019 by the IAEE. All rights reserved.

**Figure 3: An Illustrative Structure of the Model**

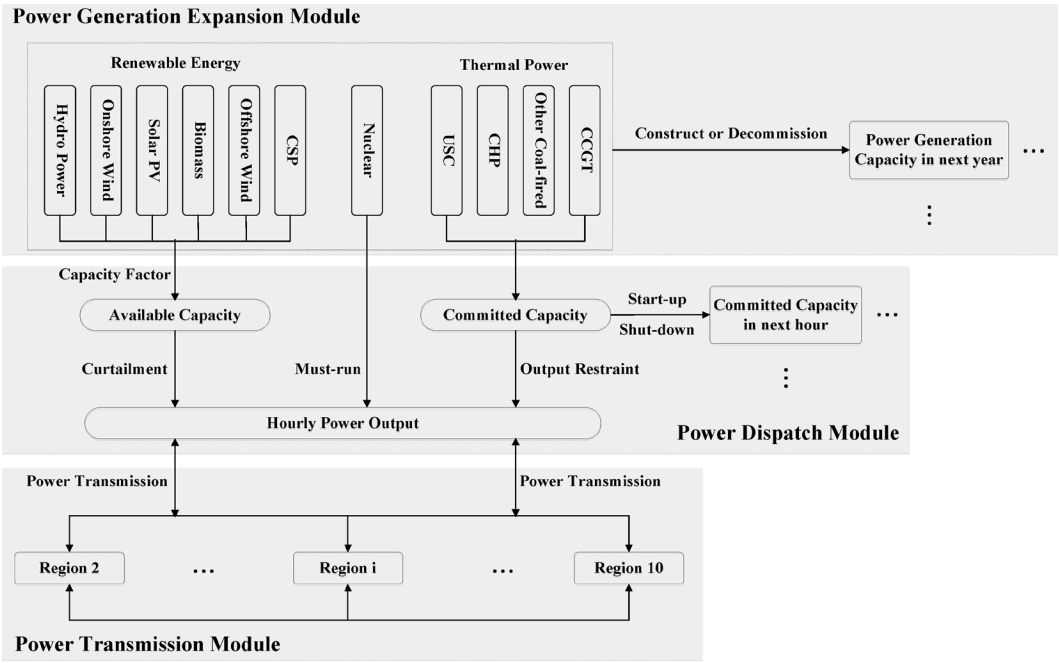


the first hour of the year are exogenously given a series of initial values according to the power outputs in the base year.

The conventional power generation technologies in the model are ultra-supercritical coal-fired power (USC), combined cycle gas turbine (CCGT), coal-fired combined heat and power (CHP), and other coal-fired power. The non-fossil power generation technologies are nuclear, hydropower, onshore wind, solar photovoltaic (PV), biomass, offshore wind, and concentrating solar power (CSP).

Ten regions are represented, characterized by geographical position, resource endowment, and power grid structure (see Table 1).[1] Each region is assumed to be a node. Consequentially, the intra-regional grid capacity restrictions or congestion is not considered. Various types of historical lines between regions are included as basic data in this model. However, for newly built lines, only ultra-high voltage direct current (UHVDC) technology is considered due to its economic advantages in long-distance power transmission (Wang, 2007).[2] In particular, ultra-high voltage alternating current (UHVAC) technology is excluded because its advantages in building a larger synchronous power grid are beyond the scope of this study.

CHP reduces flexibility of power outputs under high heating loads. Because of the central heating supply, this study assumes that CHP becomes a must-run unit during winter in five regions: the Northeast, North, Jinmengxi, Northwest, and Xinjiang. Depending on the climate, the heating

1. Xinjiang is separated from the Northwest power grid due to its remote location. Other power grids are further divided into multiple regions mainly because of the differences in resource endowments. Regional geographic distribution and resource endowment are presented in Appendix B.

2. In our previous work, the power transmission technology also includes high voltage direct current (HVDC). The results show that almost all new lines are UHVDC; therefore, this study ignores HVDC in order to simplify our model.

All rights reserved. Copyright © 2019 by the IAEE.

**Table 1: Regional Division in This Study**

| Regional symbol | Provinces, municipalities and autonomous regions included | Regional power grids |
|---|---|---|
| Northeast | Liaoning, Jilin, Heilongjiang , East Inner Mongolia | Northeast power grid |
| North | Beijing, Tianjin, Hebei, Shandong | North power grid |
| Jinmengxi | Shanxi, West Inner Mongolia | North power grid |
| Northwest | Gansu, Qinghai, Ningxia, Shaanxi | Northwest power grid |
| Xinjiang | Xinjiang | Northwest power grid |
| East | Zhejiang, Shanghai, Jiangsu, Fujian, Anhui | East power grid |
| Center | Hubei, Hunan, Jiangxi, Chongqing, Henan | Central power grid |
| Sichuan | Sichuan | Central power grid |
| South | Guangxi, Yunnan, Guizhou | Southern power grid |
| Guangdong | Guangdong | Southern power grid |

duration varies from region to region. In the North, Jinmengxi, and Northwest heating covers two typical days, while in the Northeast and Xinjiang regions it covers three typical days.

*3.1.2. Mathematical Equations*

The mathematical equations related to the unit commitment module include objective function, ramp-up and ramp-down restrictions, reserves restrictions, start-up costs, and power output restriction. The formulations related to the generation expansion planning module were discussed in Yi et al. (2016) and are presented in Appendix A.

This model is a large-scale linear programming (LP) problem solved by the CPLEX algorithm embedded in the software platform of General Algebraic Modeling System (GAMS).[3] CPLEX is chosen due to its significantly short computation time when solving large-scale LP problems.

The traditional method used in unit commitment models simulates each unit individually, which, due to limited computational capability, is not suitable when capacity expansion is also modelled for large-scale power systems. Here, generation units are grouped by technology, which could significantly reduce the amount of the commitment state for generation units. Kirchhoff's first law, the conservation of currents in each node of the power transmission network, is respected in our model, while the voltage law is not included.

The dynamics of unit commitment states for fossil fuel technology are shown in Eq. (1). The capacity of committed technology is determined by start-up and shut-down decisions.

$$U_{i,n,t,h} = U_{i,n,t,h-1} + SU_{i,n,t,h} - SD_{i,n,t,h} \quad \forall n \in N^{TP} \tag{1}$$

where the subscripts $i$, $n$, $t$, $h$ represent region, technology, year, and hour respectively; $N$ represents the set of generation technologies; the superscript $TP$ represents thermal power technologies; $U_{i,n,t,h}$ represents the committed capacity; $SU_{i,n,t,h}$ represents the capacity which starts up at time $h$ in year $t$; and $SD_{i,n,t,h}$ represents the capacity that shuts down at time $h$ in year $t$.

The maximum and minimum power output constraints for the committed technology are shown in Eq. (2).

$$U_{i,n,t,h} * P_n^{\min} \le P_{i,n,t,h} \le U_{i,n,t,h} * P_n^{\max} \quad \forall n \in N^{TP} \tag{2}$$

3. Our previous model is a nonlinear programming model that incorporates a coal transportation module. In this study, the coal transport module is replaced by exogenous coal prices in order to simplify our model into a linear programming problem.

Copyright © 2019 by the IAEE. All rights reserved.

where $P_{i,n,t,h}$ represents the power output and $P_n^{\max}$, $P_n^{\min}$ represent maximum and minimum power output rates respectively.

The ramping up and ramping down of constraints for generation units are shown in Eq. (3) and Eq. (4), respectively. If a generation unit is started up in time *h*, its power output in time *h* is assumed to equal its technical minimum output. If a generation unit is shut down in time *h*, its power output in time *h-1* is also assumed to equal its technical minimum output.

$$P_{i,n,t,h+1} - P_{i,n,t,h} \le (U_{i,n,t,h+1} - SU_{i,n,t,h+1}) * \Delta P_n^{up} + SU_{i,n,t,h+1} * P_n^{\min} - SD_{i,n,t,h+1} * P_n^{\min} \ \forall n \in N^{TP} \quad (3)$$

$$P_{i,n,t,h} - P_{i,n,t,h+1} \le (U_{i,n,t,h+1} - SU_{i,n,t,h+1}) * \Delta P_n^{down} + SD_{i,n,t,h+1} * P_n^{\min} - SU_{i,n,t,h+1} * P_n^{\min} \ \forall n \in N^{TP} \quad (4)$$

where $\Delta P_n^{up}$, $\Delta P_n^{down}$ represent the maximum ramping up and down capability.

The available capacity constraint for thermal power and nuclear is shown in Eq. (5). The committed capacity per hour in year *t* needs to be less than the total capacity determined at the beginning of year *t*. This model allows CCGT and other coal-fired power to provide reserves, so the committed capacity also needs to eliminate the capacity for spinning reserve ($SP_{i,n,t,h}$) and non-spinning reserve ($NSP_{i,n,t,h}$). For renewable energy technologies, the power output depends not only on the yearly capacity, but also on the hourly capacity factor, as shown in Eq. (6). The power outputs of renewable energy can be less than their available capacity to reflect curtailment (*CUR*) during certain hours. These two equations reflect the link between the power generation expansion module and the power dispatch module.

$$U_{i,n,t,h} \le \begin{cases} TC_{i,n,t} * ava_n - SP_{i,n,t,h} - NSP_{i,n,t,h} \ \forall n \in N^{SC\&GAS} \\ TC_{i,n,t} * ava_n \ \forall n \in N^{USC\&CHP\&NC} \end{cases} \quad (5)$$

$$CUR_{i,n,t,h} = TC_{i,n,t} * cf_{i,n,h} - P_{i,n,t,h} \ge 0 \ \forall n \in N^{RE} \quad (6)$$

where the superscript *SC*, *GAS*, *USC*, *CHP*, *NC* and *RE* represent other coal-fired power, CCGT, USC, coal-fired CHP, nuclear power and renewable energy, respectively; $TC_{i,n,t}$ represents the total capacity; $ava_n$ represents the available generation capacity rate, which does not include the units that are in a state of routine maintenance; and $cf_{i,n,h}$ represents the capacity factor for renewable energy technology.

CSP plants could be regarded as electricity storage facilities, so their modeling is different from other renewable power generation technologies.[4] The captured thermal energy can either be used directly in the steam turbine or stored in the thermal storage. This requires more explicit decisions about the utilization of solar resources (see Eqs. (7)–(9)).

$$P_{i,csp,t,h}^{direct} + P_{i,csp,t,h}^{store} = TC_{i,csp,t} * cf_{i,csp} \quad (7)$$

$$P_{i,csp,t,h} = P_{i,csp,t,h}^{direct} + P_{i,csp,t,h}^{out} \quad (8)$$

$$STO_{i,csp,t,h} = STO_{i,csp,t,h-1} * \partial_{csp} + P_{i,csp,t,h}^{store} - P_{i,csp,t,h}^{out} \quad (9)$$

4. Our model assumes that a CSP plant has a six hour storage system.

All rights reserved. Copyright © 2019 by the IAEE.

where $P^{direct}_{i,csp,t,h}$ represents electricity generated in the CSP with heat directly from the collectors; $P^{store}_{i,csp,t,h}$ represents electric equivalent of the thermal inflow into the storage; $P^{out}_{i,csp,t,h}$ represents electricity generated in the CSP with heat from the storage; $STO_{i,csp,t,h}$ represents aggregated electricity stored in time $h$; and $\partial_{csp}$ represents energy loss factor by storing.

Operating reserves are required to respond to short-term fluctuations in load, and equipment failure, including spinning reserve and non-spinning reserve. The total credit capacity at each temporal step should be larger than the demand (*PD*) plus a safety reserve, as shown in Eq. (10). This model holds a base reserve of 10 percent of load and a variable reserve equal to 10 percent of the wind and solar PV outputs in each hour, at least half of which is spinning, referring to He et al. (2016), as shown in Eq. (11). Variable reserves are required to address the uncertainty imposed by intermittent renewable energy generation. A sensitivity analysis on the variable reserves is presented in Appendix C.

$$\sum_{n\in NI} TC_{i,n,t} * ava_n + \sum_{n\in I} TC_{i,n,t} * cc_n + SPTI_{i,t,h} - SPTO_{i,t,h} \geq (1 + RC_{i,t,h}) * PD_{i,t,h} \tag{10}$$

$$\sum_{n\in SC\cup GAS} SP_{i,n,t,h} + STO_{i,csp,t,h} \geq \frac{1}{2} * RC_{i,t,h} * PD_{i,t,h} \tag{11}$$

where *NI* and *I* represent the sets of non-intermittent generators and intermittent generators, respectively; $cc_n$ represents the capacity credit rate; $SPTI_{i,t,h}$ represents the total electricity transmitted to region $i$; $SPTO_{i,t,h}$ represents the total electricity transmitted from region $i$; and $RC_{i,t,h}$ represents the reserve capacity rate, which is calculated as a percentage of regional power load plus intermittent renewable energy output.

At each time step, power demand for all regions must be met by power supply, which consists of power generation from local power plants and net inter-regional power exchange, as shown in Eq. (12).

$$PD_{i,t,h} = SPTI_{i,t,h} - SPTO_{i,t,h} + \sum_n P_{i,n,t,h} \tag{12}$$

In terms of the heat balance, this model only considers the heat generated by CHP for China's central heating supply, as shown in Eq. (13). Heat generated by boilers is assumed to remain at the base year level. The matching of regional heat supply and demand is at the level of year due to the lack of data on the hourly heat demand curve. Inter-regional heat transfer is ignored because of its huge losses.

$$\sum_h P_{i,chp,t,h} * \gamma * hpc + HGB_i \geq HD_{i,t} \tag{13}$$

where $HD_{i,t}$ represents the total central heating demand; $HGB_i$ represents the heat supplied by boilers; $\gamma$ represents the energy conversion coefficient; *hpc* represents the heat to power ratio, which is set to 0.7 based on the average level in base year (CEPYEB, 2015).

The extra cost of fossil fuel-based technologies for electricity dispatch is reflected in the start-up cost. It can be calculated as:

$$SUC_t = \sum_i \sum_n \sum_h (SU_{i,n,t,h} * C^{startup}_n) \tag{14}$$

where $SUC_t$ represents total start-up costs and $C^{startup}_n$ represents the unit start-up costs.

Copyright © 2019 by the IAEE. All rights reserved.

The objective function is to minimize the accumulated total costs of the Chinese power sector from the perspective of a social planner. Total costs (*TPC*) include investment cost ($IC_t$), operation and maintenance (O&M) cost ($OMC_t$), fuel cost ($EC_t$) of power generation technologies, the investment cost ($TIC_t$) and O&M cost ($TOMC_t$) of power transmission technologies, and the start-up and $CO_2$ emissions cost ($COC_t$), as shown in Eq. (15).

$$TPC = \sum_t (IC_t + OMC_t + EC_t + TIC_t + TOMC_t + SUC_t + COC_t) \quad (15)$$

### 3.2. Data

The data inputs related to the unit commitment module include hourly load curve, capacity factor for renewable energy, ramp-up rates, and start-up costs. Other data entering the generation expansion planning module, including power demand projection, the generation mix of existing technologies, technical and economic parameters for power transmission, distance between regions, energy price, and carbon price, are presented in Appendix B (CEPYEB, 2015; Yi et al., 2016).

#### *3.2.1. Demand Profiles*

Given that hourly power demand data in China is not publicly available, we reconstruct demand profiles from available data that capture important features of the load curve, including seasonal and daily variability for each region. The load curves for summer and winter typical days are shown in Figure 4 (Shu et al., 2005; Lai and Hong, 2007; Wei et al., 2010; Tang and Dong, 2012; Lv et al., 2013; Cheng et al., 2015). Based on monthly load characteristics, we fill in gaps by assuming continuity in load profiles and interpolating values for other typical days. One limitation of our model is that it assumes a constant load curve shape in the future. The corresponding load behavior changes are not considered.

**Figure 4: Typical Daily Load Curves in 2014 in China**

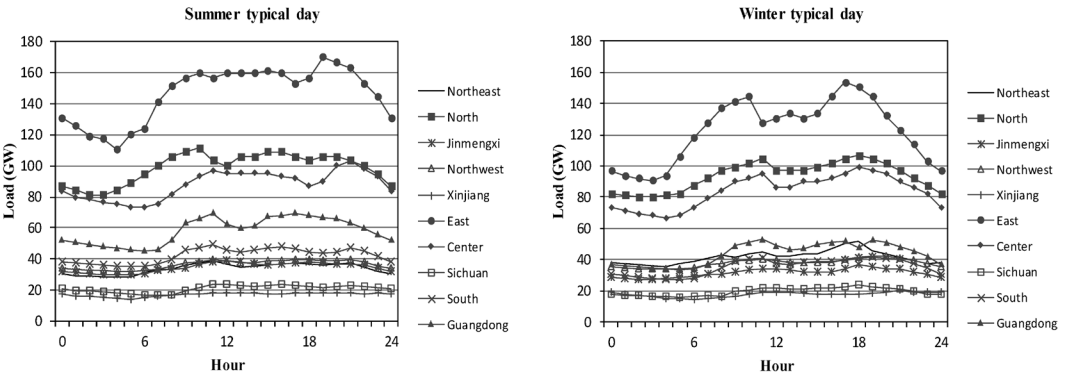


#### *3.2.2. Meteorological Data for Renewable Energy*

The hourly capacity factors of solar PV and CSP are based on the PVWatts tool and the System Advisor Model from the National Renewable Energy Laboratory (NREL), which estimates the solar resource resources at a given location.

The hourly capacity factors of onshore and offshore wind are calculated as follows. First, the wind speed data within a six-hour interval is collected from Kalnay et al. (1996), which includes

All rights reserved. Copyright © 2019 by the IAEE.

the wind resources at a given location. Second, lagrange interpolation is done to adjust the six-hour interval to hourly wind speed data. Third, a deterministic wind power curve for 2.5 MW turbine is used to convert wind speed into capacity factors of wind power (Zhu and Genton, 2012). Finally, the data are calibrated based on regional average capacity factors in 2016 (NEA, 2017).

Hydropower generation depends on natural rainfall inflows, which vary significantly between seasons. Monthly capacity factors for different regions are from Li et al. (2016). The hourly availability of hydropower is assumed to be the same for a given typical day.

Detailed capacity factors of solar PV, onshore wind, and hydropower at the hourly level are presented in Appendix B.

*3.2.3. Key Technical and Economic Parameters*

Key technical and economic parameters for the power generation technologies, investment cost, O&M cost, start-up cost, maximum power output, minimum power output, ramping up rate, and ramping down rate, are shown in Table 2.

**Table 2: Technical and Economic Parameters for Power Generation Technologies**

| Technology | Investment cost (RMB/KW) [b] | O&M cost (RMB/KW)[b] | Start-up cost (RMB/time/KW)[c] | Maximum power output rate (%)[c] | Minimum power output rate (%)[c] | Ramping up rate (%/h)[c] | Ramping down rate (%/h)[c] |
|---|---|---|---|---|---|---|---|
| USC | 3915 | 290 | 0.70 | 100 | 40 | 10 | 10 |
| CCGT | 2830 | 80 | 0.25 | 100 | 25 | 40 | 40 |
| CHP | 4090 | 350 | 0.42 | 100 | 40 [d] | 10 | 10 |
| Other coal-fired | 4880 | 300 | 0.42 | 100 | 40 | 10 | 10 |
| Nuclear[a] | 15500 | 1000 | – | – | – | – | – |
| Hydro | 10000 | 46 | – | – | – | – | – |
| Onshore wind | 7750 | 253 | – | – | – | – | – |
| Solar PV | 8600 | 128 | – | – | – | – | – |
| Biomass | 10470 | 300 | – | – | – | – | – |
| Offshore wind | 13000 | 600 | – | – | – | – | – |
| CSP | 20000 | 250 | – | – | – | – | – |

*Notes:* The symbol "–" means that the data those are not needed in this model.

[a] This study assumes that the output of nuclear power is always at the maximum level.

[b] Yi et al. (2016), Davidson et al. (2016), Cheng et al. (2015), Yi et al. (2017).

[c] Li et al. (2016), Koltsaklis and Georgiadis (2015).

[d] During winter time, the minimum power output rate of CHP in the north of China is assumed to increase to 55%, referring to Davidson et al. (2016).

### 3.3. Scenario Design

Based on the stylized analysis in Section 2, we find the coal-heavy generation mix (notably CHP) and inter-regional electricity trade significantly affect regional renewable energy development. Therefore, we investigate how to deploy renewable energy at the spatial level to achieve low-carbon targets through six counter-factual scenarios structured along these two dimensions. First, we consider exogenously changing the regional CHP capacity to reflect the extent of the coal-heavy generation mix. The following three cases are chosen to represent the future level of CHP capacity:

(1) *Base* assumes the regional CHP capacities remain at the 2014 level. No new capacity will be built during the planning horizon.

(2) *BAU* refers to the projection of the increase of CHP capacity from Davidson et al. (2016). The total CHP capacity in 2030 will reach 385 GW, a 36% increase compared to the base year.

Copyright © 2019 by the IAEE. All rights reserved.

(3) *Double* assumes that the growth rate of CHP is twice that of the BAU scenario, with a total capacity of 487 GW in 2030, to reflect a higher level of coal-heavy generation mix.

A second dimension explores the role of the inter-regional power transmission grid on electricity trade. The following two cases are chosen to represent the future level of the transmission network:

(1) *Frozen* assumes Chinese inter-regional transmission infrastructure remains at the 2014 level. No new infrastructure will be built during the planning horizon.
(2) *Optimal* assumes no restrictions on inter-regional transmission infrastructure construction between any regions. The optimal transmission network during the planning horizon is endogenously calculated by our model.

Two policy targets are assumed to promote renewable energy. The first is that the share of non-fossil energy in total primary energy in 2030 is 20% ($\lambda_{pet}$), as indicated in the U.S.-China Joint Announcement on Climate Change (see Eq. (16)). The second is that the share of non-hydro renewable energy in total power generation in 2030 is 17% ($\lambda_{rps}$), referring to Yi et al. (2017), as shown in Eq. (17).[5]

$$\sum_{i}\sum_{n\in NFF}\sum_{h}P_{i,n,2030,h} \geq PEC_{2030} * \lambda_{pet} \tag{16}$$

$$\sum_{i}\sum_{n\in NHR}\sum_{h}P_{i,n,2030,h} \geq \sum_{i}\sum_{n}\sum_{h}P_{i,n,2030,h} * \lambda_{rps} \tag{17}$$

where the set *NFF* and *NHR* represent non-fossil energy and non-hydro renewable energy respectively; $PEC_{2030}$ represents the total primary energy consumption in 2030.

## 4. MODELING RESULTS

### 4.1. Optimal Renewable Energy Spatial Deployment

Figure 5 shows the regional power generation from non-hydro renewable energy in the *Optimal+BAU* scenario in 2030. We take this scenario as the analysis object in this section because it represents the most likely situation. Not surprisingly, the share of onshore wind in the renewable energy generation mix is the largest, reaching 63.9%. It is followed by solar PV, which generates 316 TWh in 2030, accounting for 22.1% of renewable electricity. Power generations from biomass, offshore wind, and CSP remain relatively small, accounting for 6.5%, 4.1%, and 3.4%, respectively.

There is a serious regional imbalance in the spatial deployment of non-hydro renewable energy. 75.7% is from the north of China, which includes the Northeast, North, Jinmengxi, Northwest, and Xinjiang regions. The increase rates in the Northwest and Xinjiang are relatively higher, leading to a nine-fold increase in 2030 compared with 2014. The non-hydro renewable energy in the south of China is mainly from the East, followed by the Center and South regions. Sichuan shows the fastest relative growth, but its absolute amount remains low.

The difference in resource endowments are the main reason for this imbalance. Both onshore wind and solar PV resources are concentrated in the north of China, especially in the North-

5. Non-hydro renewable energy includes onshore wind, offshore wind, biomass, CSP, and solar PV.

All rights reserved. Copyright © 2019 by the IAEE.

**Figure 5: Regional Power Generation from Non-hydro Renewable Energy**

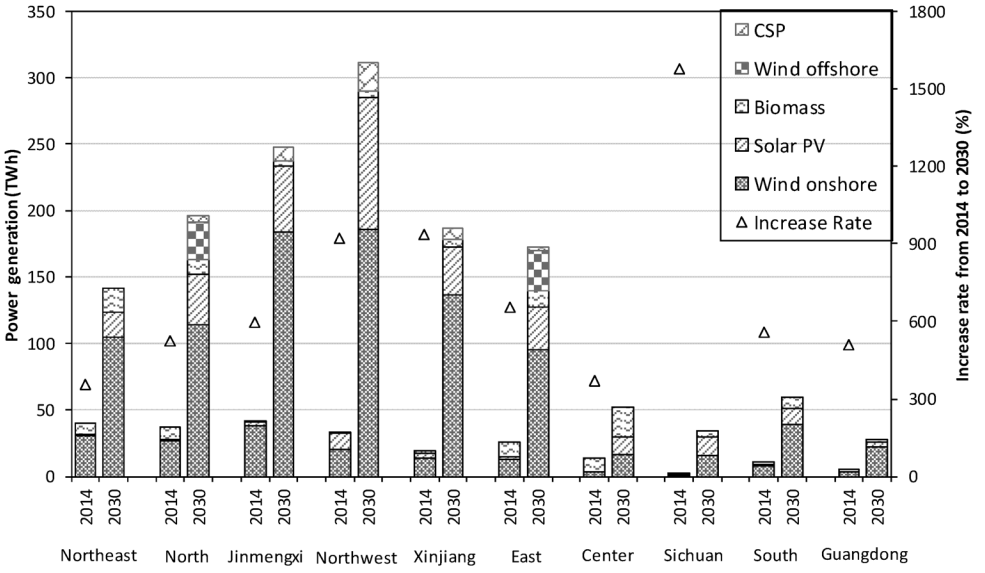


west, Xinjiang, and Jinmengxi regions. Only biomass and offshore wind are largely located in the central and south of China, but their absolute volumes are limited.

### 4.2. Impact Factors of Renewable Energy Spatial Deployment

Before our analysis, we characterized the regions by two dimensions. First, from the view of geographic location, we define the Northeast, North, Jinmengxi, Northwest, and Xinjiang regions as "the north of China," while the other five regions are defined as "the south of China." This is because the central heating supply in the north of China affects the utilization mode of CHP significantly in the winter. Second, from the view of resource endowment of non-hydro renewable energy, we define the Northeast, Jinmengxi, Northwest, and Xinjiang regions as "resource-rich" areas, while the other six are defined as "resource-poor" areas. Figs. 8 and 9 show the renewable energy generation changes from the dimensions of both coal-heavy generation mix and inter-regional power transmission.

#### *4.2.1. Coal-heavy Generation Mix*

With the increase in CHP capacity, renewable energy deployment shifts from the north of China to the south of China. This trend is alleviated with inter-regional power transmission. As shown in Figure 6, when CHP capacity is at the *Double* level, renewable energy production in the south of China increases by 59 TWh in the *Frozen* scenario, but increases by only 27 TWh in the *Optimal* scenario.

Not all regions in the north of China are affected by CHP capacity changes. The most affected regions include Northeast, North, and Jinmengxi, while renewable energy production in Northwest and Xinjiang regions vary little, as the shares of CHP in these two regions are relatively small. For the north of China, power transmission could mitigate the transfer of renewable energy caused by high CHP capacity both in resource-rich and resource-poor areas. For the resource-rich

Copyright © 2019 by the IAEE. All rights reserved.

**Figure 6: Non-hydro RE Changes under Different CHP Levels in 2030**

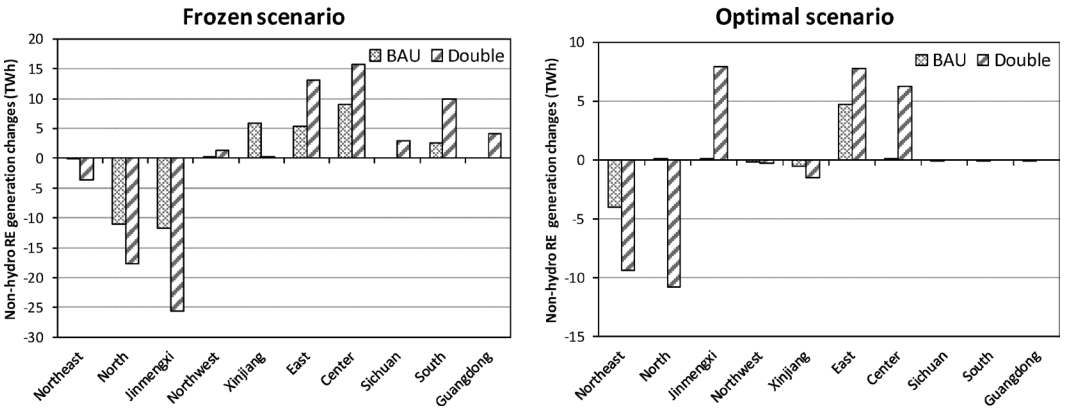


***Notes***: Base scenario is seen as the benchmark. These changes are obtained by the results in the BAU scenario and Double scenario minus those in the Base scenario. Detail results for regional non-hydro RE generation in 2030 are shown in Appendix C.

areas, such as Jinmengxi, there are a large number of transmission lines connected to the East and Center regions. Excessive thermal power can be exported to the load center to provide more space for local renewable energy. For resource-poor areas such as the North region, little electricity is exported, but power transmission leads to a reduction in renewable energy production, which makes it less susceptible to the change of base load.

*4.2.2. Inter-regional Power Transmission*

With the increase of inter-regional power transmission, renewable energy deployment shifts from resource-poor to resource-rich areas, and this trend is more significant in high CHP scenarios. As shown in Figure 7, if the construction of inter-regional transmission lines is allowed, the renewable energy production in resource-rich areas increases by 44 TWh in the *Base* scenario, and reaches 69 TWh in the *Double* scenario. Because all resource-rich areas are located in the north of China, the above-mentioned rule that power transmission could lower the transfer of renewable energy caused by high CHP capacity is still applicable here.

Among the resource-rich areas, the Northwest region is most affected by inter-regional power transmission. Although it has the most abundant renewable energy resources, it has fewer power transmission lines in the base year, so the excess renewable energy could not be consumed in the *Frozen* scenario. While the Xinjiang region, which also has abundant natural resources, is almost unaffected due to geographical factors, it gains little from power transmission compared to the Northwest and Jinmengxi, as it is far from load centers like the Center and East. Among resource-poor areas, renewable energy production rises slightly in the Sichuan and South, which are rich in hydropower. Power transfer could further promote surplus hydropower consumption, leading to more space for other renewable energies.

*4.2.3. Decomposition Effects*

Onshore wind and solar PV are used to explore the effects of the coal-heavy generation mix and inter-regional power transmission on the power structure of non-hydro renewable energy. Tables 3 and 4 present the capacity of onshore wind and solar PV in 2030 from the perspective of

All rights reserved. Copyright © 2019 by the IAEE.

**Figure 7: Non-hydro RE Changes under Inter-regional Power Transfer in 2030**

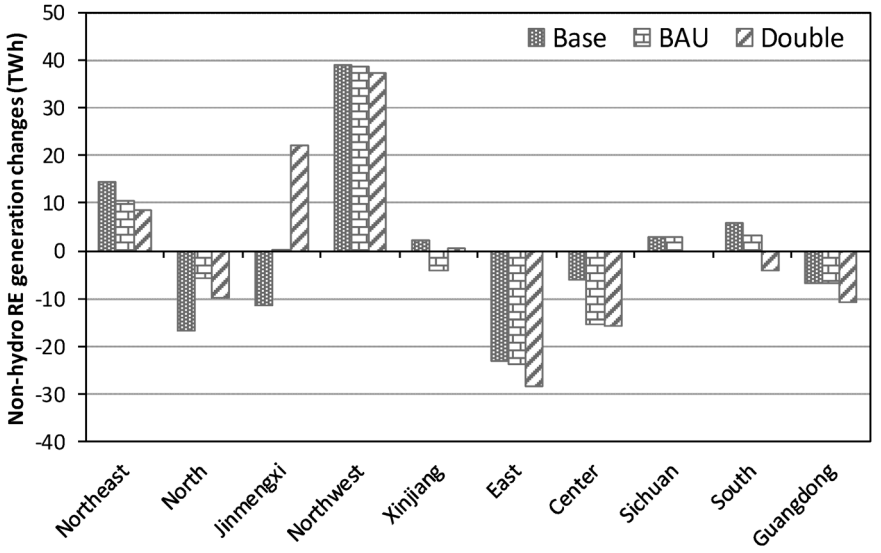


***Notes***: *Frozen* scenario is seen as the benchmark. These changes are obtained by the results in the *Optimal* scenario minus those in the *Frozen* scenario.

**Table 3: Capacity of Onshore Wind and Solar PV in 2030 from a Geographic Location View**

| | Onshore Wind | | | | | | Solar PV | | | | | |
|---|---|---|---|---|---|---|---|---|---|---|---|---|
| | Frozen | | | Optimal | | | Frozen | | | Optimal | | |
| Region (GW) | Base | BAU | Double | Base | BAU | Double | Base | BAU | Double | Base | BAU | Double |
| The north of China | 310.5 | 302.2 | 295.6 | 336.3 | 334.1 | 328.7 | 194.6 | 200.3 | 204.6 | 172.5 | 172.5 | 178.2 |
| The south of China | 109.3 | 111.5 | 116.9 | 106.4 | 106.4 | 106.4 | 81.0 | 81.0 | 92.6 | 63.4 | 67.6 | 77.4 |
| National total | 419.8 | 413.7 | 412.5 | 442.7 | 440.5 | 435.1 | 275.6 | 281.3 | 297.2 | 235.9 | 240.1 | 255.6 |

**Table 4: Capacity of Onshore Wind and Solar PV in 2030 from a Resource Endowment View**

| | Onshore Wind | | | | | | Solar PV | | | | | |
|---|---|---|---|---|---|---|---|---|---|---|---|---|
| | Base | | BAU | | Double | | Base | | BAU | | Double | |
| Region (GW) | Frozen | Optimal | Frozen | Optimal | Frozen | Optimal | Frozen | Optimal | Frozen | Optimal | Frozen | Optimal |
| Resource-rich areas | 254.3 | 280.1 | 251.0 | 277.9 | 245.9 | 277.9 | 151.1 | 143.0 | 157.5 | 143.0 | 159.6 | 148.7 |
| Resource-poor areas | 165.5 | 162.6 | 162.7 | 162.6 | 166.6 | 157.2 | 124.5 | 92.9 | 123.8 | 97.1 | 137.6 | 106.9 |
| National total | 419.8 | 442.7 | 413.7 | 440.5 | 412.5 | 435.1 | 275.6 | 235.9 | 281.3 | 240.1 | 297.2 | 255.6 |

both geographic location and resource endowment. Detailed results at the regional level are shown in Appendix C.

High CHP capacity induces an increase of solar PV and a decrease of onshore wind. The inverse relationship between wind power and electricity demand makes it more susceptible to an increase in the base load. The decrease of onshore wind is mainly in the north of China, especially in the North and Jinmengxi regions, which are highly affected by CHP. In turn, the increase of solar PV is primarily found in the south of China. The increase in must-run capacity is, to a certain extent,

Copyright © 2019 by the IAEE. All rights reserved.

not conducive to the utilization of solar PV in the north of China. In addition, surplus wind power is transmitted to the south of China, which has a negative impact on the utilization of local wind power.

Through the analysis of the power supply structure, we find that transfers of renewable energy deployment caused by high CHP capacity are mainly reflected in the reduction of onshore wind in the north of China and the rise of solar PV in the south of China.

Inter-regional power transmission could lead to a significant increase in onshore wind and a decrease of solar PV. The increase in wind power occurs in the resource-rich areas, while the reduction of solar PV mainly comes from resource-poor areas, although a small percentage is in the resource-rich areas. Inter-regional transmission could lead to more efficient power dispatch, which is equivalent to improving the utilization space for renewable energy in resource-rich areas. Thus, greater amounts of onshore wind power are deployed there due to its relatively low generation cost.

The transfer of renewable energy deployment caused by inter-regional power transmission is mainly reflected in the reduction of solar PV in resource-poor areas and an increase of onshore wind in resource-rich areas.

### 4.3. Renewable Energy Curtailment

Table 5 shows the renewable energy curtailment rate during the planning horizon.[6] It is highest in the Northeast region; other relatively high areas are Jinmengxi, Xinjiang, Sichuan, and South. The high CHP capacity induces an increase in the curtailment rate, particularly in the north of China, while inter-regional power transmission could reduce it across almost every region.

**Table 5: Renewable Energy Curtailment During the Planning Horizon**

| | Frozen | | | Optimal | | |
|---|---|---|---|---|---|---|
| Region (%) | Base | BAU | Double | Base | BAU | Double |
| Northeast | 7.20 | 8.06 | 11.66 | 3.51 | 3.61 | 4.64 |
| North | 0.03 | 0.01 | 0.82 | 0.01 | 0.04 | 0.01 |
| Jinmengxi | 1.76 | 2.01 | 3.09 | 0.81 | 0.86 | 0.89 |
| Northwest | 0.93 | 1.05 | 1.39 | 0.48 | 0.45 | 0.42 |
| Xinjiang | 1.07 | 1.40 | 1.64 | 0.93 | 1.12 | 1.27 |
| East | 0.49 | 0.48 | 0.43 | 0.05 | 0.03 | 0.03 |
| Center | 0.03 | 0.05 | 0.04 | 0.06 | 0.05 | 0.05 |
| Sichuan | 3.65 | 4.03 | 4.61 | 0.13 | 0.14 | 0.14 |
| South | 1.85 | 1.87 | 1.81 | 0.16 | 0.16 | 0.14 |
| Guangdong | 0.07 | 0.05 | 0.55 | 0.00 | 0.00 | 0.00 |
| National average | 1.81 | 2.00 | 2.46 | 0.43 | 0.45 | 0.49 |

*Notes:* This curtailment rate is the sum of hydro power, onshore wind, offshore wind, and solar PV during the planning horizon.

The sources of renewable energy curtailment differ across regions. In the Northeast, Jinmengxi, and Xinjiang regions, it is primarily wind power that is curtailed, mainly due to the lack of flexibility in power dispatch caused by increased CHP capacity. Meanwhile, hydropower is generally curtailed in Sichuan and South regions. These two areas have abundant hydropower resources, which are not only difficult for the local demand to consume, but also to some extent compress the

6. The results of our simulation are lower than the current curtailment rate in China. This is because our study does not consider the uncertainty of renewable energy or intra-regional power congestion. In addition, the matching between power supply and demand is based on a perfect system perspective, which can also lead to a reduction in curtailment rate. Nonetheless, we can still find the patterns of the changes by comparing various scenarios.

All rights reserved. Copyright © 2019 by the IAEE.

space for other renewable energy sources. The existing transmission channels are unable to meet the utilization of excess resources.

### 4.4. Optimal Inter-regional Transmission Grid

Figure 8 shows the volume of optimal inter-regional power transmission flows in 2030.[7] The *BAU* scenarios show a significant increase in inter-regional power flow in the *Optimal* case, reaching 1,449 TWh in 2030, 2.4 times higher than the *Frozen* case. The total capacity of inter-regional power transmission infrastructure reaches 347 GW by 2030. The infrastructure built during 2015–2030 accounts for 214 GW. Electricity export volumes increase significantly in the Jinmengxi, Northwest, and Sichuan regions, while electricity import volumes increase significantly in East, Center, and Guangdong.

It is necessary to coordinate transmission infrastructure extension planning and renewable energy deployment in order to minimize system costs and reduce curtailment. However, transmission grids are not exclusively used to promote the consumption of renewable energy. For example, in the Jinmengxi region, a large percentage of electricity from cheap coal power plants is exported. Thus, the average annual utilization rates of these lines are relatively high, between 50%–67%. In contrast, electricity exports from Sichuan are primarily from hydropower, and inter-regional power transmission leads to an increase in generation of 40%. Electricity exports from the Northwest come from both wind and thermal power. This combination allows for a high utilization rate of the lines, which is at around 55%, thus improving the economy of electricity transmission. The Northwest-East and Northwest-Center patterns of electricity transmission play an important role in the consumption of wind power.

Increasing CHP capacity induces excessive thermal power in the north of China. As a result, more transmission infrastructure connecting the north and the south of China are constructed, such as Jinmengxi-East, Jinmengxi-Center, and Northwest-Center. In the *Double* scenario, the electricity transfers between north and south increase by approximately 29% compared with the *Base* scenario.

### 4.5. Cost Analysis

Table 6 shows cost decomposition during the planning horizon. Increasing inter-regional power transmission can lead to a significant reduction in the total production cost in the power sector. In the *BAU* case, total costs fall by 2.9%, and the absolute amount is 903.5 billion RMB during 2015–2030.[8] Part of the cost reduction is explained by the transfer of coal consumption from high-price to low-price regions. Cost reduction is also explained by the higher utilization of coal-fired power. More flexible dispatching can increase a unit's annual operation hours to avoid unnecessary investment. Increased CHP capacity leads to an increase in the total cost in the given framework, but because it also provides heating supply, cost effectiveness cannot be accurately analyzed from the perspective of the power sector alone.

We also find that inter-regional power transmission induces higher carbon emissions. The main driver of this result is that power transmission increases economic incentives to export cheap low-efficiency coal-fired electricity. It can also be attributed to our assumption that all scenarios

7. As the power transmission networks in all *Frozen* scenarios remain at the level of base year, the differences of power flow between each are very small. Therefore, we only present the results of the *Frozen+BAU* scenario.

8. All costs in this study are 2014 constant price.

Copyright © 2019 by the IAEE. All rights reserved.

**Figure 8: Optimal Inter-regional Power Transmission in 2030 (TWh)**

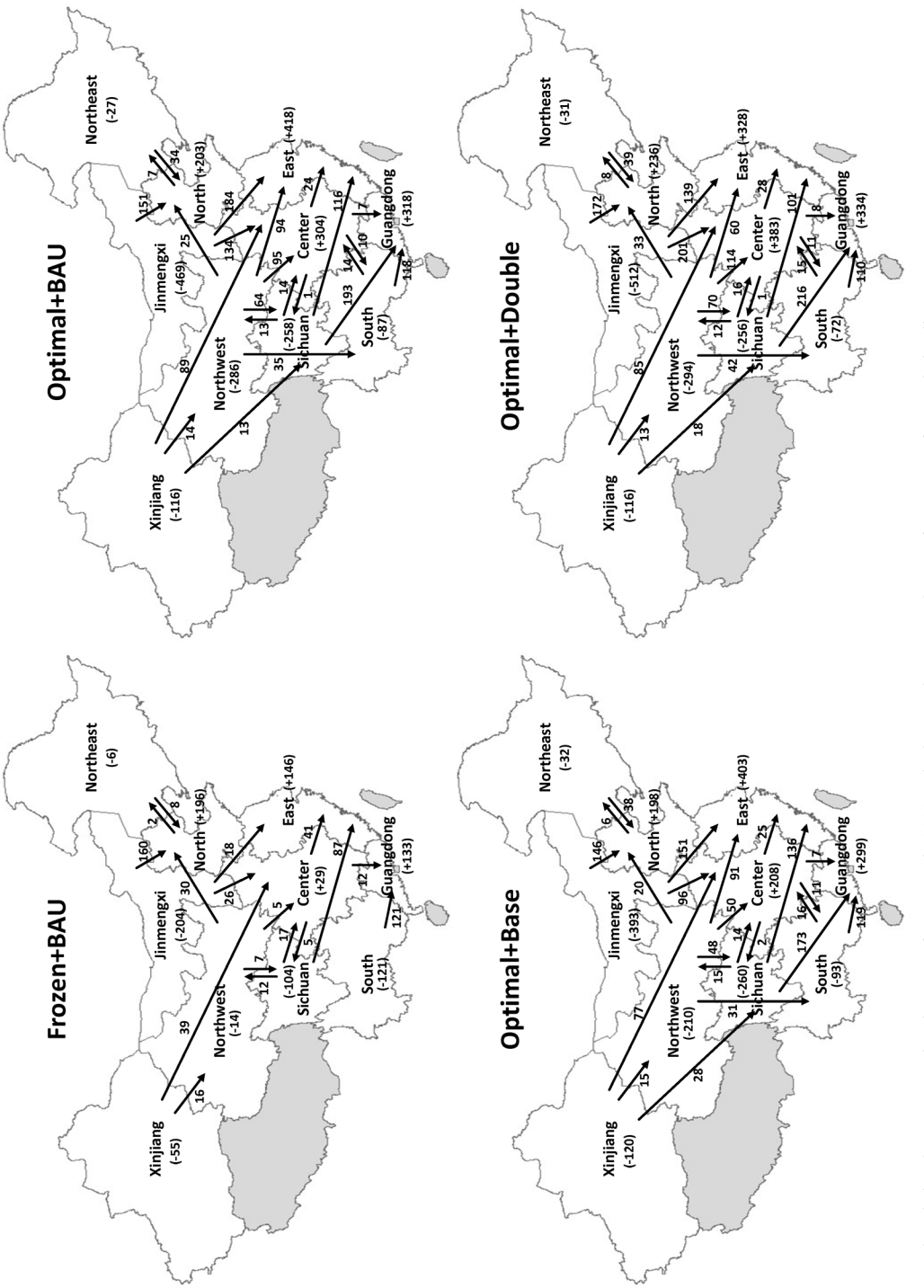


*Notes*: The numbers in brackets mean regional net transfer amount in 2030 and other numbers mean the transfer amount of transmission line.

All rights reserved. Copyright © 2019 by the IAEE.

**Table 6: Costs Decomposition During the Planning Horizon**

| | Frozen | | | Optimal | | |
|---|---|---|---|---|---|---|
| Costs (Billion RMB) | Base | BAU | Double | Base | BAU | Double |
| Investment cost for power generation | 7,607.9 | 7,643.2 | 7,832.2 | 7,114.8 | 7,138.4 | 7,187.7 |
| O&M cost for power generation | 8,604.6 | 8,673.8 | 8,811.1 | 8,160.1 | 8,219.6 | 8,276.5 |
| Investment cost for power transmission | 0.0 | 0.0 | 0.0 | 362.8 | 402.3 | 416.9 |
| O&M cost for power transmission | 137.3 | 140.5 | 143.5 | 242.4 | 262.9 | 271.7 |
| Start-up cost | 225.6 | 230.4 | 228.0 | 152.4 | 157.1 | 161.2 |
| Energy consumption cost | 14,322.0 | 14,371.8 | 14,365.5 | 13,991.7 | 13,925.3 | 13,923.5 |
| $CO_2$ emission cost | 320.3 | 337.1 | 340.6 | 370.8 | 387.7 | 403.6 |
| Total costs | 31,217.7 | 31,396.8 | 31,720.9 | 30,395.0 | 30,493.3 | 30,641.1 |
| Total generation costs for non-hydro renewable energy | 5,015.7 | 5,042.5 | 5,181.6 | 4,946.1 | 4,963.5 | 4,973.7 |

need to achieve the same renewable energy production target; therefore, fossil-based electricity is not replaced by clean renewable energy in the *Optimal* case. High CHP capacity also induces an increase of carbon emissions. Most CHPs in China are 300 MW large-capacity units and due to the lack of nearby heating demand, the efficiency of such units is lower than that of ultra-supercritical coal-fired power units.

The renewable energy deployment changes caused by high CHP capacity induce an increase in the total generation cost of non-hydro renewable energy, especially under current levels of the transmission network. However, optimal inter-regional transmission network extensions reduce this cost by 1.6% in the *BAU* case, and the absolute amount is 79 billion RMB. Additionally, the start-up cost could partially reflect the cost of thermal power for adapting fluctuating characteristics of renewable energy. Inter-regional transmission is more conducive to the temporal dispatch of electricity, reducing about 30% of start-up costs.

## CONCLUSIONS

This paper integrates short-term unit commitment into a long-term generation expansion planning framework to develop a multi-regional power sector optimization model for China. Based on this model, we quantitatively analyze the optimal spatial deployment of renewable energy in China to achieve relevant low-carbon targets, and compare the impact of a coal-heavy generation mix and inter-regional electricity transmission on the spatial deployment of renewable energy.

Our analysis highlights the central role played by the north of China in achieving low-carbon policy targets. Approximately 75% of non-hydro renewable energy should be deployed in these regions under the least-cost cases. The share of onshore wind in the non-hydro renewable energy generation mix is the largest, reaching 63.9% in 2030. It is followed by solar PV, which accounts for 22.1% of renewable electricity.

Another significant finding is that the deployment of renewable energy depends on the regional power structure and inter-regional power transmission network. With an increase of combined heat and power (CHP), more renewable energy facilities, especially solar PV, should be located in the south of China because of the conflict between CHP and onshore wind in the north of China. In contrast, an optimal inter-regional transmission network is beneficial to onshore wind production in resource-rich areas, and induces a transfer of renewable energy deployment from resource-poor areas to resource-rich areas.

The scale of CHP primarily depends on the surrounding heat demand. Excessive CHP capacity increases the total generation costs for achieving the national non-hydro renewable energy

Copyright © 2019 by the IAEE. All rights reserved.

target, because it leads to an increase in the curtailment rate of renewable energy, particularly in the north of China. An enhanced inter-regional power transmission network is crucial because, on the one hand, it can cope with the significant regional imbalance of energy resources and electricity load; on the other hand, it can mitigate the conflict between the coal-heavy generation mix and renewable energy. It also has the potential to bring sizeable gains from electricity trade, estimated to be 4.4–11.7 billion RMB per year, which would help reach the energy targets.

Our findings also point to the need to consider the coordination between inter-regional transmission infrastructure planning and the spatial deployment of renewable energy. The Northwest-East and Northwest-Center patterns of electricity transmission play a key role in the consumption of onshore wind power. Our analysis demonstrates that intra-regional power network planning must keep pace with the development of renewable energy. Reducing intra-regional electricity congestion is the premise that inter-regional power transmission can bring the benefits in reducing renewable energy curtailment and generation costs.

This article is the first step in developing a power sector optimization model that integrates unit commitment with generation expansion planning framework based on the Chinese power sector. Our work suggests several directions for future research. First, the consideration for the uncertainty of intermittent renewable energy is not enough in this study. Stochastic models for dealing with uncertainties were widely used in unit commitment problems (Wang and Hobbs, 2016; Warrington et al., 2016; Morales-España et al., 2017). But when short-term unit commitment is combined with long-term large-scale capacity expansion, computational feasibility will be the main difficulty in applying stochastic models to cope with the uncertainty of renewable energy. Second, heating systems other than CHP can be integrated into the power sector optimization model to analyze the interaction between electricity systems and heating systems. Data collections of hourly heat demand curve and existing heat boiler, heat pump, and heat storage capacities in China will be the main challenges for such an expansion.

## ACKNOWLEDGMENTS

This work is supported by the National Key Research and Development Program of China under Grant No. 2017YFE0101800, the National Natural Science Foundation of China under Grant No. 71690245, No. 71673266, No. 71403263 and Beijing Natural Science Foundation under Grant No. 9152019. The authors appreciate the weekly joint seminars at CEEP in CAS and Beihang SEM, from where the earlier draft of the paper got improved.

## REFERENCES

Abrell, J. and S. Rausch (2016). "Cross-country electricity trade, renewable energy and European transmission infrastructure policy." *Journal of Environmental Economics and Management* 79: 87–113. https://doi.org/10.1016/j.jeem.2016.04.001.

Bertsch, J., T. Brown, S. Hagspiel, and L. Just (2017). "The relevance of grid expansion under zonal markets." *The Energy Journal* 38(5): 129–152. https://doi.org/10.5547/01956574.38.5.jber.

Bird, L., C. Chapman, J. Logan, J. Sumner, and W. Short (2011). "Evaluating renewable portfolio standards and carbon cap scenarios in the US electric sector." *Energy Policy* 39(5): 2573–2585. https://doi.org/10.1016/j.enpol.2011.02.025.

Chang, Y. and Y. Li (2015). "Renewable energy and policy options in an integrated ASEAN electricity market: Quantitative assessments and policy implications." *Energy Policy* 85: 39–49. https://doi.org/10.1016/j.enpol.2015.05.011.

Chen, Z., L. Ma, P. Liu, and Z. Li (2018). "Electric vehicle development in China: A charging behavior and power sector supply balance analysis." *Chemical Engineering Research and Design* 131: 671–685. https://doi.org/10.1016/j.cherd.2017.11.016.

All rights reserved. Copyright © 2019 by the IAEE.

Cheng, L., Y. Feng, and N. Wang (2015). "Load characteristics analysis and peak margin calculation of Beijing-Tianjin-Northern Hebei power grid." *North China Electric Power* 11: 1–5 (in Chinese).

Cheng, R., Z. Xu, P. Liu, Z. Wang, Z. Li, and L. Jones (2015). "A multi-region optimization planning model for China's power sector." *Applied Energy* 137: 413–426. https://doi.org/10.1016/j.apenergy.2014.10.023.

China Electric Power Yearbook Editorial Board (CEPYEB) (2015). "China electric power yearbook 2015." Beijing: *China Electric Power Press* (in Chinese).

Davidson, M.R., D. Zhang, W. Xiong, X. Zhang, and V. Karplus (2016). "Modelling the potential for wind energy integration on China's coal-heavy electricity grid." *Nature Energy* 1, 16086. https://doi.org/10.1038/nenergy.2016.86.

Dong, L., H. Liang, Z. Gao, X. Luo, and J. Ren (2016). "Spatial distribution of China's renewable energy industry: Regional features and implications for a harmonious development future." *Renewable and Sustainable Energy Reviews* 58: 1521–1531. https://doi.org/10.1016/j.rser.2015.12.307.

Egerer, J., C. Gerbaulet, C. and Lorenz (2016). "European electricity grid infrastructure expansion in a 2050 context." *The Energy Journal* 37(SI3): 101–124. https://doi.org/10.5547/01956574.37.SI3.jege.

Egerer, J., J. Rosellon, and W.P. Schill (2015). "Power system transformation toward renewables: an evaluation of regulatory approaches for network expansion." *The Energy Journal* 36(4): 105–128. https://doi.org/10.5547/01956574.36.4.jege.

Guo, Z., R. Cheng, Z. Xu, P. Liu, Z. Wang, Z. Li, L. Jones, and Y. Sun (2017). "A multi-regional load dispatch model for the long-term optimum planning of China's electricity sector." *Applied Energy* 185: 556–572. https://doi.org/10.1016/j.apenergy.2016.10.132.

He, G, A.P. Avrin, J.H. Nelson, J. Johnston, A. Mileva, J. Tian, and D.M. Kammen (2016). "SWITCH-China: a systems approach to decarbonizing China's power system." *Environmental Science & Technology* 50(11): 5467–5473. https://doi.org/10.1021/acs.est.6b01345.

Kaleta, M. and E. Toczyłowski (2008). "Restriction techniques for the unit-commitment problem with total procurement costs." *Energy Policy* 36(7): 2439–2448. https://doi.org/10.1016/j.enpol.2008.01.039.

Kalnay et al. (1996). "The NCEP/NCAR 40-year reanalysis project." *Bull. Amer. Meteor. Soc.* 77: 437–470. https://doi.org/10.1175/1520-0477(1996)077<0437:TNYRP>2.0.CO;2.

Keane, A., A. Tuohy, P. Meibom, E. Denny, D. Flynn, A. Mullane, and M. O'Malley (2011). "Demand side resource operation on the Irish power system with high wind power penetration." *Energy Policy* 39(5): 2925–2934. https://doi.org/10.1016/j.enpol.2011.02.071.

Koltsaklis, N.E. and M.C. Georgiadis (2015). "A multi-period, multi-regional generation expansion planning model incorporating unit commitment constraints." *Applied Energy* 158: 310–331. https://doi.org/10.1016/j.apenergy.2015.08.054.

Lai, M. and B. Hong (2007). "The influences of the air conditioning load on the daily load characteristics of Central China power grid." *Electric Power Technologic Economics* 19(3): 30–33 (in Chinese).

Li, Y. and Y. Chang (2015). "Infrastructure investments for power trade and transmission in ASEAN+ 2: Costs, benefits, long-term contracts and prioritized developments." *Energy Economics* 51: 484–492. https://doi.org/10.1016/j.eneco.2015.08.008.

Li, Y., Z. Lukszo, and M. Weijnen (2016). "The impact of inter-regional transmission grid expansion on China's power sector decarbonization." *Applied Energy* 183: 853–873. https://doi.org/10.1016/j.apenergy.2016.09.006.

Lienert, M. and S. Lochner (2012). "The importance of market interdependencies in modeling energy system–The case of the European electricity generation market." *Electrical Power and Energy Systems* 34: 99–113. https://doi.org/10.1016/j.ijepes.2011.09.010.

Lv, Q., W. Wang, S. Han, S. Yuan, J. Zhang, and W. Li (2013). "A new evaluation method for wind power curtailment based on analysis of system regulation capability." *Power System Technology* 37(7): 1887–1894 (in Chinese).

Ministry of Housing and Urban-Rural Development of the People's Republic of China (MOHURD) (2015). *China urban construction statistical yearbook 2014*. Available from http://www.mohurd.gov.cn/xytj/tjzljsxytjgb/jstjnj/index.html.

Moarefdoost, M.M., A.J. Lamadrid, and L.F. Zuluaga (2016). "A robust model for the ramp-constrained economic dispatch problem with uncertain renewable energy." *Energy Economics* 56: 310–325. https://doi.org/10.1016/j.eneco.2015.12.019.

Morales-Espa-a, G., L. Ramírez-Elizondo, and B.F. Hobbs (2017). "Hidden power system inflexibilities imposed by traditional unit commitment formulations." *Applied Energy* 191: 223–238. https://doi.org/10.1016/j.apenergy.2017.01.089.

National Energy Administration (NEA) (2017). "Wind power generation situation in 2016." Available from http://www.nea.gov.cn/2017-01/26/c_136014615.htm (in Chinese).

Pei, W., Y. Chen, K. Sheng, W. Deng, Y. Du, Z. Qi, and L. Kong (2015). "Temporal-spatial analysis and improvement measures of Chinese power system for wind power curtailment problem." *Renewable and Sustainable Energy Reviews* 49: 148–168. https://doi.org/10.1016/j.rser.2015.04.106.

Perez, A.P., E.E. Sauma, F.D. Munoz, and B.F. Hobbs (2016) "The economic effects of interregional trading of renewable energy certificates in the U.S. WECC." *The Energy Journal* 37(4): 267–296. https://doi.org/10.5547/01956574.37.4.aper.

Copyright © 2019 by the IAEE. All rights reserved.

Pfluger, B. (2014). "Assessment of least-cost pathways for decarbonising Europe's power supply: A model-based long-term scenario analysis accounting for the characteristics of renewable energies." KIT Scientific Publishing, Karlsruhe, Germany.

Scholz, Y., H.C. Gils, and R.C. Pietzcher (2017). "Application of a high-detail energy system model to derive power sector characteristics at high wind and solar shares." *Energy Economics* 64: 568–582. https://doi.org/10.1016/j.eneco.2016.06.021.

Shu, J., J. Zhang, and Y. Zheng (2005). "Discussion on rational scale of pumped storage power station in East China power grid in 2010." *Water Resources and Power* 23(5): 54–57 (in Chinese).

Sullivan, P., C. Uriarte, and W. Short (2014). "Greenhouse gas mitigation options in the U.S. electric sector: a ReEDS analysis." *The Energy Journal* 35(1): 101–114. https://doi.org/10.5547/01956574.35.SI1.6.

Tang, B. and Z. Dong (2012). "Analysis on load characteristics of China southern power grid in 11th Five Year Plan." *Electric Power* 45(10): 30–35 (in Chinese).

Wang, B., and B.F. Hobbs (2016). "Real-time markets for flexiramp: A stochastic unit commitment-based analysis." *IEEE Transactions on Power Systems* 31(2): 846–860. https://doi.org/10.1109/TPWRS.2015.2411268.

Wang, Z. (2007). "Economy and security analysis of AC UHV in China." *Electric Power Automation Equipment* 27(10): 1–4 (in Chinese).

Warrington, J., C. Hohl, P. Goulart, and M. Morari (2016). "Rolling unit commitment and dispatch with multi-stage recourse policies for heterogeneous devices." *IEEE Transactions on Power Systems* 31(1): 187–197. https://doi.org/10.1109/TPWRS.2015.2391233.

Wei, L., L. Zhang, and N. Jiang (2010). "Analysis of load characteristics for Northwest China power grid." *Power System and Clean Energy* 26(7): 57–62 (in Chinese).

Weigt, H., D. Ellerman, and E. Delarue (2013). "$CO_2$ abatement from renewables in the German electricity sector: Does a $CO_2$ price help?" *Energy Economics* 40: 149–158. https://doi.org/10.1016/j.eneco.2013.09.013.

Wright, E. and A. Kanudia (2014). "Low carbon standard and transmission investment analysis in the new multi-region U.S. power sector model FACETS." *Energy Economics* 46: 136–150. https://doi.org/10.1016/j.eneco.2014.09.013.

Xinhua News Agency (XNA) (2014). "U.S.-China joint announcement on climate change." Available from: http://www.xinhuanet.com/video/2014-11/13/c_127205443.htm (in Chinese).

Yi, B., J. Xu, and Y. Fan (2016). "Inter-regional power grid planning up to 2030 in China considering renewable energy development and regional pollutant control: A multi-region bottom-up optimization model." *Applied Energy* 184: 641–658. https://doi.org/10.1016/j.apenergy.2016.11.021.

Yi, B., J. Xu, and Y. Fan (2017). "Optimal pathway and impact of achieving the mid-long term renewable energy standard in China." *Journal of Systems Engineering* 32(3): 313–324 (in Chinese).

Yi, B., J. Xu, and Y. Fan (2019). "Coordination of policy goals between renewable portfolio standards and carbon caps: A quantitative assessment in China." *Applied Energy* 237: 25–35. https://doi.org/10.1016/j.apenergy.2018.12.015.

Zhang, D., J. Wang, Y. Lin, Y. Si, C. Huang, J. Yang, B. Huang, and W. Li (2017). "Present situation and future prospect of renewable energy in China." *Renewable and Sustainable Energy Reviews* 76: 865–871. https://doi.org/10.1016/j.rser.2017.03.023.

Zhu, X., and M. Genton (2012). "Short-term wind speed forecasting for power system operations." *International Statistical Review* 80(1): 2–23. https://doi.org/10.1111/j.1751-5823.2011.00168.x.

## APPENDIX A: MATHEMATICAL EQUATIONS

### A.1 Power generation module

The calculation of the total capacity of each technology is shown in Eq. (1). Every power generation technology will be decommissioned at the end of its expected lifetime.

$$TC_{i,n,t} = \sum_{t'=t-T_n+1}^{t} NC_{i,n,t'} \tag{1}$$

where the subscripts $i$, $n$, $t$ represent region, technology, and year respectively; $T_n$ represents the lifetime of technology (y); $TC_{i,n,t}$, $NC_{i,n,t}$ represent the total capacity, and the new capacity of technology $n$ in year $t$ respectively (MW).

All rights reserved. Copyright © 2019 by the IAEE.

The investment cost is discounted equally to each year of its lifetime. It means if the lifetime of the technology exceeds the planning horizon, investment cost is scaled down to consider the residual value. The calculation is shown in Eq. (2).

$$IC_t = \sum_i \sum_n \left[ \sum_{t'=t-T_n+1}^{t} \left( CAP_{n,t'} \cdot NC_{i,n,t'} \cdot \frac{I \cdot (1+I)^{-1}}{1-(1+I)^{-T_n}} \right) \right] \tag{2}$$

where $IC_t$ represents the total investment cost in year $t$ (RMB); $CAP_{n,t}$ represents the unit investment cost of technology in year $t$ (RMB/MW); $I$ represents the discount rate to reflect the expected return rate of investment (%), which is 10% in this model (Yi et al., 2016).

The fixed operation and maintenance (O&M) cost can be calculated as follow:

$$OMC_t = \sum_i \sum_n TC_{i,n,t} \cdot COM_{n,t} \tag{3}$$

where $OMC_t$ represents the total O&M cost in year $t$ (RMB); $COM_{n,t}$ represents the unit O&M cost (RMB/MW).

Fuel cost is proportional to the price and consumption rate of each kind of fuel. Fuels used in power sector include the coal, natural gas, biomass, and uranium. It is a major variable cost in the power generation process, calculated as follow:

$$EC_t = \sum_i \sum_n \sum_h (P_{i,n,t,h} \cdot es_n + SP_{i,n,t,h} \cdot spes_n) \cdot ep_{i,n,t} \tag{4}$$

where the subscript $h$ represents hour; $EC_t$ represents the total energy consumption cost in year $t$ (RMB); $P_{i,n,t,h}$ represents the power output of technology $n$ at time $h$ in year $t$ (MWh); $es_n$ represents the energy consumption per unit of electricity (t/MWh); $SP_{i,n,t,h}$ represents the capacity for spinning reserve at time $h$ in year $t$ (MW); $spes_n$ represents the unit energy consumption for spinning reserve (t/MW); $ep_{i,n,t}$ represents the energy price (RMB/t).

The emission trading scheme will be introduced in this model. A carbon cap (the upper limit for annual $CO_2$ emissions of the power sector) and a $CO_2$ price are assumed for each year. If the $CO_2$ emissions exceed this cap, it needs to buy allowances from the carbon market. On the other hand, it can also sell its superfluous allowances to get revenue. The $CO_2$ price is exogenous. The detailed calculations are shown in Eqs. (5)–(6).

$$TCE_t = \sum_i \sum_n \sum_h P_{i,n,t,h} \cdot es_n \cdot \theta_n \tag{5}$$

$$COC_t = pco_t \cdot (TCE_t - ET_t) \tag{6}$$

where $TCE_t$ represents the total $CO_2$ emissions in year $t$ (t-$CO_2$); $\theta_n$ represents the unit $CO_2$ emission of the fuel used by technology $n$ (t-$CO_2$/t); $COC_t$ represents the total $CO_2$ emission cost (or revenue) in year $t$ (RMB); $pco_t$ represents the $CO_2$ price (RMB/t-$CO_2$); $ET_t$ represents the $CO_2$ cap in year $t$ (t-$CO_2$).

The annual generation capacity expansion can be constrained by factors such as labors, materials, and capability of facilities manufacturing, a certain value is set for the annual construction speed of each type of power generation technology, as presented by Eq. (7).

$$NC_{i,n,t} \leq MaxNB_{i,n} \tag{7}$$

where $MaxNB_{i,n}$ represents the maximum expansion allowed within one year (MW).

Copyright © 2019 by the IAEE. All rights reserved.

**A.2 Power transmission module**

The calculation of the total capacity of each transmission technology is shown in Eq. (8). Every power transmission technology will be decommissioned at the end of its expected lifetime.

$$TTC_{i,j,t} = \sum_{t'=t-T+1}^{t} TNC_{i,j,t'} \tag{8}$$

where the subscript $j$ also represent region; $TTC_{i,j,t}$, $TNC_{i,j,t}$ represent the total capacity, and the new capacity of transmission technology in year $t$ respectively (MW).

The investment cost of power transmission technology consists of two parts: the fixed costs and variable costs. Among them, the variable costs are proportional to the transmission distance. It is also discounted equally to each year of its lifetime. The calculation is shown in Eq. (9).

$$TIC_t = \sum_i \sum_j \left[ \sum_{t'=t-T+1}^{t} \left( \left( TFCAP_{t'} + TVCAP_{t'} \cdot dis_{i,j} \right) \cdot TNC_{i,j,t'} \cdot \frac{I \cdot (1+I)^{-1}}{1-(1+I)^{-T}} \right) \right] \tag{9}$$

where $dis_{i,j}$ represents the distance between region $i$ and $j$ (km); $TIC_t$ represents the total investment cost of power transmission technology (RMB); $TFCAP_t$ represents the unit fix investment cost of power transmission technology in year $t$ (RMB/MW); $TVCAP_t$ represents the unit variable investment cost of power transmission technology in year $t$ (RMB/km/MW).

The total O&M cost of power transmission technology can be calculated as follow:

$$TOMC_t = \sum_i \sum_i TTC_{i,j,t} \cdot TCOM_{i,j} \tag{10}$$

where $TOMC_t$ represents the total O&M cost of power transmission technology in year $t$ (RMB); $TCOM_{i,j}$ represents the unit O&M cost of power transmission technology (RMB/MW).

At each time step, power demand for all regions should be met by power supply, which consists of power generation from local power plants, and net inter-regional power exchange, as shown in Eqs. (11)-(13).

$$PD_{i,t,h} = SPTI_{i,t,h} - SPTO_{i,t,h} + \sum_n P_{i,n,t,h} \tag{11}$$

$$SPTI_{i,t,h} = \sum_j^{j \neq i} PT_{j,i,t,h} \cdot \left(1 - ptl_{j,i}\right) \tag{12}$$

$$SPTO_{i,t,h} = \sum_i^{i \neq j} PT_{i,j,t,h} \tag{13}$$

where $PD_{i,t,h}$ represents power demand in time $h$ (MWh); $SPTI_{i,t,h}$ represents the total electricity transmitted to region $i$ in time $h$ (MWh); $SPTO_{i,t,h}$ represents the total electricity transmitted from region $i$ in time $h$ (MWh); $ptl_{i,j}$ represents the transmission loss between region $i$ and $j$ (%); $PT_{i,j,t,h}$ represents the electricity transmitted from region $i$ to $j$ (MWh).

Electricity traded within any hour should be subject to the constraint of available transmission capacity, as shown in Eq. (14).

$$PT_{i,j,t,h} \leq TTC_{i,j,t} \cdot avatr \tag{14}$$

where $avatr$ represents the available transmission capacity rate (%).

All rights reserved. Copyright © 2019 by the IAEE.

## APPENDIX B: DATASETS

### B.1 Demand projection

**Table B1: Power demand projection during the planning horizon**

| | Northeast | North | Jinmengxi | Northwest | Xinjiang | East | Center | Sichuan | South | Guangdong |
|---|---|---|---|---|---|---|---|---|---|---|
| Growth rate of power demand during 2015–2020 (%) | 4.9 | 4.5 | 4.5 | 6.8 | 6.8 | 4.3 | 5.3 | 5.3 | 4.9 | 4.9 |
| Growth rate of power demand during 2020–2030 (%) | 2.4 | 2.2 | 2.2 | 3.0 | 3.0 | 2.0 | 2.4 | 2.4 | 2.2 | 2.2 |

Source: Yi et al. (2016).

The central heating demand projections during the planning horizon are from the Building Energy Research Center of Tsinghua University. This total demand is decomposed into each region based on the heat consumption structure in the base year (MOHURD, 2015).

**Table B2: Central heating demand projection**

| Region (Million GJ) | 2015 | 2020 | 2025 | 2030 |
|---|---|---|---|---|
| Northeast | 1066 | 1153 | 1266 | 1376 |
| North | 995 | 1076 | 1182 | 1284 |
| Jinmengxi | 292 | 316 | 348 | 378 |
| Northwest | 201 | 217 | 238 | 259 |
| Xinjiang | 152 | 165 | 181 | 197 |
| East | 123 | 133 | 146 | 158 |
| Center | 89 | 97 | 106 | 115 |
| Sichuan | 0 | 0 | 0 | 0 |
| South | 0 | 0 | 0 | 0 |
| Guangdong | 0 | 0 | 0 | 0 |

### B.2 Generation mix of existing technologies

**Table B3: Regional installed capacity of power generation technologies until 2014 (GW)**

| | Northeast | North | Jinmengxi | Northwest | Xinjiang | East | Center | Sichuan | South | Guangdong |
|---|---|---|---|---|---|---|---|---|---|---|
| SC | 12.5 | 21.5 | 8.7 | 5.0 | 3.0 | 94.2 | 43.5 | 0.0 | 4.4 | 20.0 |
| CCGT | 0.6 | 9.1 | 2.1 | 0.7 | 0.2 | 26.3 | 2.9 | 0.2 | 0.2 | 11.6 |
| CHP | 54.5 | 77.6 | 42.5 | 15.7 | 8.8 | 63.7 | 18.5 | 1.4 | 0.0 | 0.0 |
| Other coal-fired | 16.9 | 29.8 | 51.7 | 40.4 | 23.3 | 38.2 | 62.8 | 14.3 | 50.8 | 34.1 |
| Nuclear | 2.0 | 0.0 | 0.0 | 0.0 | 0.0 | 10.9 | 0.0 | 0.0 | 0.0 | 7.3 |
| Hydro power | 8.1 | 3.5 | 3.3 | 22.5 | 5.9 | 26.8 | 66.9 | 62.6 | 89.0 | 13.1 |
| Onshore wind | 23.0 | 16.2 | 17.1 | 15.5 | 7.7 | 5.8 | 2.3 | 0.3 | 5.3 | 2.2 |
| Solar PV | 0.6 | 1.5 | 2.8 | 11.4 | 3.3 | 3.6 | 0.6 | 0.1 | 0.3 | 0.5 |
| Biomass | 1.6 | 1.8 | 0.1 | 0.2 | 0.4 | 2.3 | 2.0 | 0.1 | 0.4 | 0.4 |
| Offshore wind | 0.0 | 0.0 | 0.0 | 0.0 | 0.0 | 0.6 | 0.0 | 0.0 | 0.0 | 0.0 |
| CSP | 0.0 | 0.0 | 0.0 | 0.0 | 0.0 | 0.0 | 0.0 | 0.0 | 0.0 | 0.0 |

Sources: Yi et al. (2016); CEPYEB (2015).

Copyright © 2019 by the IAEE. All rights reserved.

**Figure B1: Regional geographic distribution and installed capacity of renewable energy in 2014**

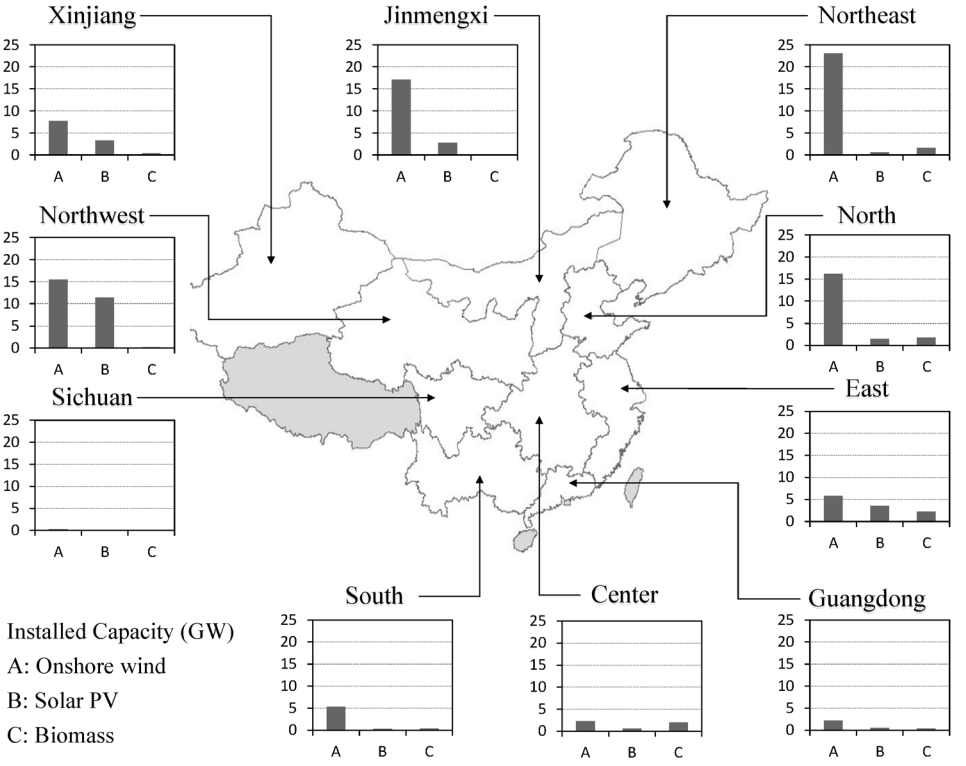


## B.3 Key technical and economic parameters for power transmission

**Table B4: Technical and economic parameters for power transmission technology**

| Technology | Fix investment cost (RMB/kW) | Variable investment cost (RMB/km/kW) | Lifetime (year) | Transmission loss (%/1000 km) | Annual decrease rate of investment cost (%) |
|---|---|---|---|---|---|
| UHVDC | 1491 | 0.786 | 40 | 2.75 | 0.01 |

Source: Yi et al. (2016).

## B.4 Distance between regions

**Table B5: Distance of inter-regional transmission lines (km)**

| | Northeast | North | Jinmengxi | Northwest | Xinjiang | East | Center | Sichuan | South | Guangdong |
|---|---|---|---|---|---|---|---|---|---|---|
| Northeast | 0 | 1078 | 1283 | 2286 | 3118 | 1940 | 2085 | 2640 | 2943 | 2773 |
| North | 1078 | 0 | 697 | 1539 | 2727 | 861 | 1006 | 1561 | 1864 | 1694 |
| Jinmengxi | 1283 | 697 | 0 | 1008 | 2049 | 1391 | 1261 | 1319 | 1836 | 1999 |
| Northwest | 2286 | 1539 | 1008 | 0 | 1370 | 1824 | 1393 | 693 | 1347 | 1952 |
| Xinjiang | 3118 | 2727 | 2049 | 1370 | 0 | 3176 | 2763 | 1958 | 2549 | 3287 |
| East | 1940 | 861 | 1391 | 1824 | 3176 | 0 | 537 | 1484 | 1451 | 935 |
| Center | 2085 | 1006 | 1261 | 1393 | 2763 | 537 | 0 | 959 | 945 | 740 |
| Sichuan | 2640 | 1561 | 1319 | 693 | 1958 | 1484 | 959 | 0 | 655 | 1334 |
| South | 2943 | 1864 | 1836 | 1347 | 2549 | 1451 | 945 | 655 | 0 | 891 |
| Guangdong | 2773 | 1694 | 1999 | 1952 | 3287 | 935 | 740 | 1334 | 891 | 0 |

Source: Authors' estimation.

All rights reserved. Copyright © 2019 by the IAEE.

## B.5 Energy prices

### Table B6: Regional energy prices in the base year

| | Northeast | North | Jinmengxi | Northwest | Xinjiang | East | Center | Sichuan | South | Guangdong |
|---|---|---|---|---|---|---|---|---|---|---|
| Coal (RMB/tce) | 518 | 522 | 370 | 377 | 346 | 608 | 571 | 604 | 587 | 703 |
| Natural gas (RMB/1000m$^3$) | 3000 | 3650 | 2800 | 2300 | 2110 | 4000 | 3600 | 3250 | 4000 | 4850 |
| Biomass (RMB/t) | 304 | 328 | 303 | 265 | 320 | 351 | 295 | 280 | 273 | 350 |

Source: Yi et al. (2016).

## B.6 Capacity factor

### Table B7: Capacity factor of hydropower

| Typical day | Northeast | North | Jinmengxi | Northwest | Xinjiang | East | Center | Sichuan | South | Guangdong |
|---|---|---|---|---|---|---|---|---|---|---|
| Day 1 | 0.171 | 0.057 | 0.114 | 0.228 | 0.205 | 0.143 | 0.177 | 0.251 | 0.200 | 0.103 |
| Day 2 | 0.278 | 0.093 | 0.186 | 0.371 | 0.334 | 0.232 | 0.288 | 0.409 | 0.325 | 0.167 |
| Day 3 | 0.471 | 0.157 | 0.314 | 0.628 | 0.565 | 0.392 | 0.486 | 0.691 | 0.549 | 0.282 |
| Day 4 | 0.514 | 0.171 | 0.342 | 0.685 | 0.617 | 0.428 | 0.531 | 0.753 | 0.599 | 0.308 |
| Day 5 | 0.407 | 0.136 | 0.271 | 0.543 | 0.488 | 0.339 | 0.420 | 0.597 | 0.475 | 0.244 |
| Day 6 | 0.214 | 0.071 | 0.143 | 0.285 | 0.257 | 0.179 | 0.221 | 0.314 | 0.250 | 0.128 |

### Figure B2: Capacity factor of solar PV

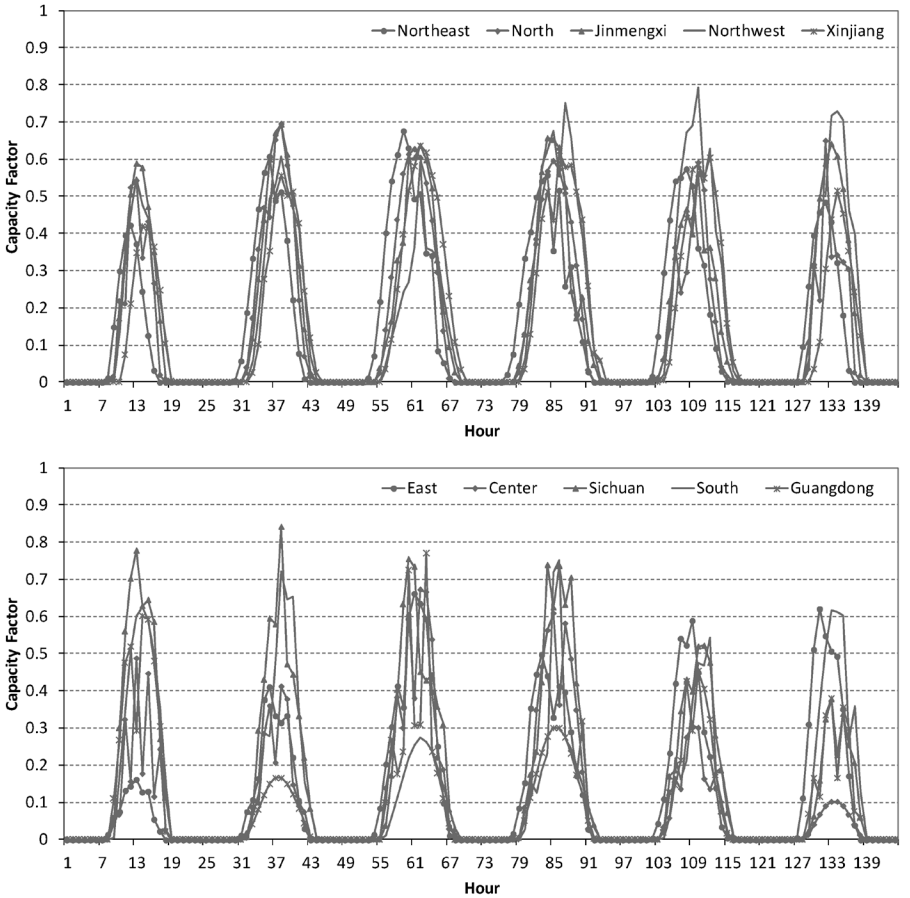


Copyright © 2019 by the IAEE. All rights reserved.

**Figure B3: Capacity factor of onshore wind**

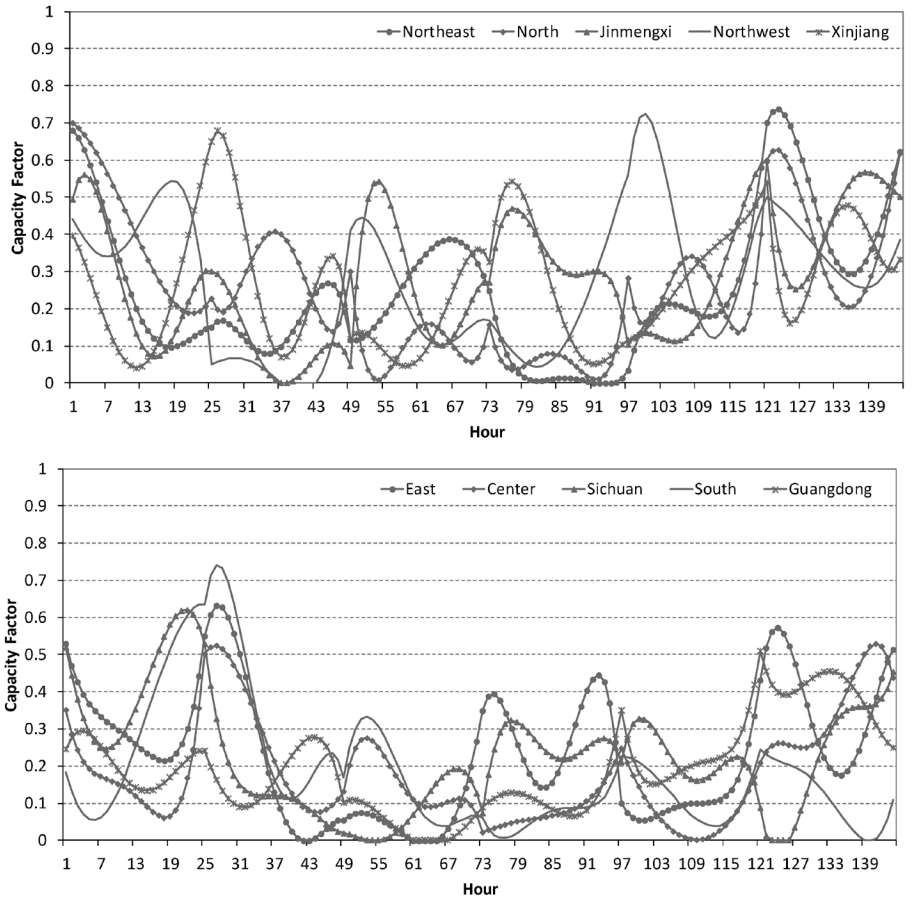


## APPENDIX C: DETAIL RESULTS

### C.1 Regional power generation mix

Figure C1 shows the regional power generation mix for 2030 in the *Optimal+BAU* scenario. The share of thermal power in total generation is the largest, reaching 53.2%. Power generation from hydropower, non-hydro renewable energy, and nuclear power remains relatively low, accounting for 18.5%, 17.0%, and 11.3%, respectively.

Our results reveal a significant regional difference in the power generation mix in 2030. Hydropower is mainly located in the Sichuan and South regions, while nuclear power is distributed in the East, Guangdong, and Center. Thermal power occupies the largest share of power generation in all regions except Sichuan, South, and Guangdong. The share of non-hydro renewable energy in regional power generation also varies greatly. This share is higher than 20% in Xinjiang, Northwest, Jinmengxi, and Northeast. However, it is lower than 10% in the South, Guangdong, Sichuan, and Center regions.

All rights reserved. Copyright © 2019 by the IAEE.

**Figure C1: Power generation mix in the "Optimal+BAU" scenario in 2030**

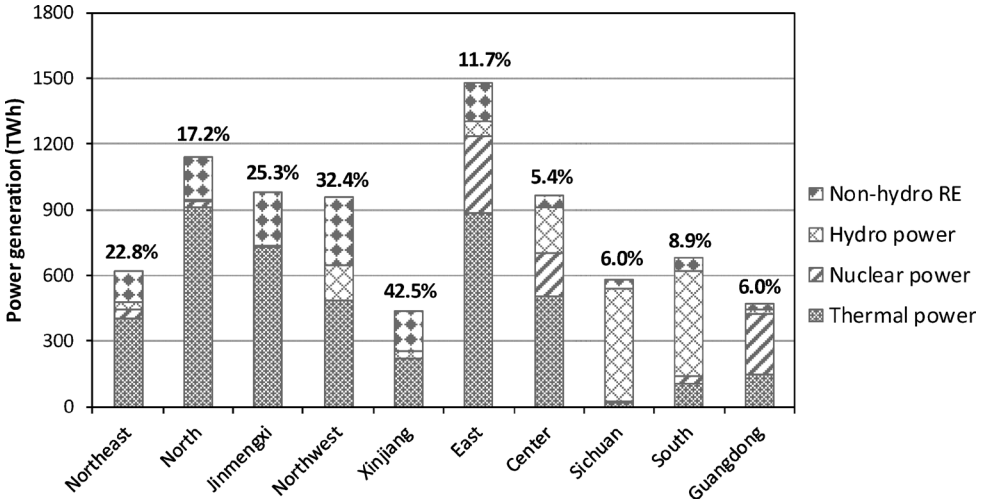


*Notes:* The numbers above the pillars represent the share of non-hydro renewable energy in regional total power generation. "RE" in the legend is the abbreviation of renewable energy.

## C.2 Regional non-hydro renewable energy generation

**Table C1: Regional non-hydro renewable energy generation in 2030**

| | Frozen | | | Optimal | | |
|---|---|---|---|---|---|---|
| Region (TWh) | Base | BAU | Double | Base | BAU | Double |
| Northeast | 131 | 131 | 127 | 145 | 141 | 136 |
| North | 213 | 202 | 195 | 196 | 196 | 185 |
| Jinmengxi | 259 | 247 | 233 | 247 | 248 | 255 |
| Northwest | 272 | 272 | 274 | 311 | 311 | 311 |
| Xinjiang | 185 | 191 | 185 | 187 | 187 | 185 |
| East | 191 | 196 | 204 | 168 | 172 | 175 |
| Center | 58 | 67 | 74 | 52 | 52 | 58 |
| Sichuan | 32 | 32 | 35 | 35 | 35 | 35 |
| South | 54 | 57 | 64 | 60 | 60 | 60 |
| Guangdong | 35 | 35 | 39 | 28 | 28 | 28 |

## C.3 Regional capacity of onshore wind and solar PV

**Table C2: Regional capacity of onshore wind and solar PV in 2030**

| | Onshore Wind | | | | | | Solar PV | | | | | |
|---|---|---|---|---|---|---|---|---|---|---|---|---|
| | Frozen | | | Optimal | | | Frozen | | | Optimal | | |
| Region (GW) | Base | BAU | Double | Base | BAU | Double | Base | BAU | Double | Base | BAU | Double |
| Northeast | 47.7 | 47.2 | 50.1 | 53.4 | 51.2 | 51.2 | 14.6 | 18.1 | 18.1 | 14.6 | 14.6 | 14.6 |
| North | 56.2 | 51.2 | 49.7 | 56.2 | 56.2 | 50.8 | 43.5 | 42.8 | 45.0 | 29.5 | 29.5 | 29.5 |
| Jinmengxi | 80.3 | 75.9 | 70.4 | 80.3 | 80.3 | 80.3 | 42.8 | 42.8 | 42.8 | 34.8 | 34.8 | 40.5 |
| Northwest | 65.9 | 65.9 | 66.7 | 83.9 | 83.9 | 83.9 | 66.3 | 66.3 | 66.3 | 66.3 | 66.3 | 66.3 |
| Xinjiang | 60.4 | 62.0 | 58.7 | 62.5 | 62.5 | 62.5 | 27.4 | 30.3 | 32.4 | 27.3 | 27.3 | 27.3 |
| East | 55.3 | 55.3 | 55.3 | 48.8 | 48.8 | 48.8 | 31.5 | 31.5 | 38.5 | 24.5 | 28.7 | 31.5 |
| Center | 10.9 | 13.1 | 13.7 | 10.9 | 10.9 | 10.9 | 21.6 | 21.6 | 21.6 | 14.6 | 14.6 | 21.6 |
| Sichuan | 8.3 | 8.3 | 8.3 | 8.3 | 8.3 | 8.3 | 8.1 | 8.1 | 10.1 | 10.1 | 10.1 | 10.1 |
| South | 19.3 | 19.3 | 22.1 | 24.9 | 24.9 | 24.9 | 13.3 | 13.3 | 15.9 | 10.7 | 10.7 | 10.7 |
| Guangdong | 15.5 | 15.5 | 17.5 | 13.5 | 13.5 | 13.5 | 6.5 | 6.5 | 6.5 | 3.5 | 3.5 | 3.5 |
| National total | 419.8 | 413.7 | 412.5 | 442.7 | 440.5 | 435.1 | 275.6 | 281.3 | 297.2 | 235.9 | 240.1 | 255.6 |

Copyright © 2019 by the IAEE. All rights reserved.

### C.4 Key sensitivity analysis

The spatial deployment of renewable energy may be influenced by many factors, including future fuel prices, cost reduction rate of technologies, and errors in renewable forecasting. Regulation uncertainties, such as environmental policy, electricity market reform, and emission trading scheme, will also impact the evolution pathway of technologies.

Based on the focus of this study, we examine three key factors: the renewable costs, the variable reserves, and the capacity factors, using the *Optimal+BAU* scenario, as shown in Figure C2. In the first case, the investment costs of wind and solar in 2030 will be 20% lower or 10% higher than the *Optimal+BAU* scenario. In the second case, the variable reserves are set to 0%, 10%, 20%, and 50% of the intermittent wind and solar outputs, respectively. These changes lead to a certain impact on system costs, and natural gas capacity. But, they have little impact on the spatial deployment of renewable energy.

In the third case, the capacity factors of wind and solar will be 10% lower or 10% higher than the *Optimal+BAU* scenario during the planning horizon. The share of non-hydro renewable energy generation in the north of China varies between 75.1% and 76.6%. The decrease of capacity factor requires more renewable units to be built, resulting in less vulnerable to the impact of the historical power structure distribution.

**Figure C2: Impacts of key factors on the spatial deployment of renewable energy**

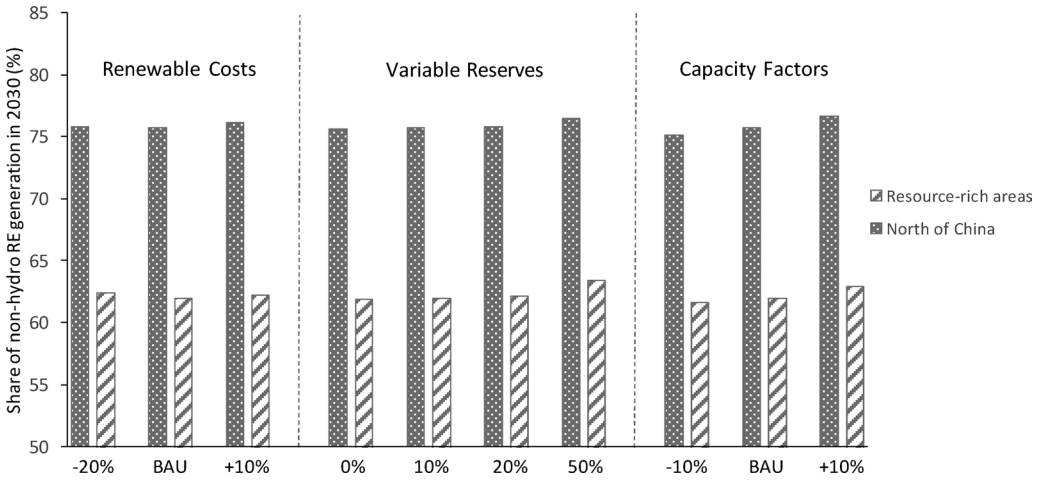


All rights reserved. Copyright © 2019 by the IAEE.